STUDY OF SHEAR STRESS ON THE SURFACE OF AN OBSTACLE ATTACHED TO WALL OF A NARROW CHANNEL

A Thesis Submitted in Partial Fulfillment of the Requirements
For the Degree of

Bachelor of Technology
in
Mechanical Engineering

Submitted by

Shivam Yadav
Roll Number – 111ME0352

Department of Mechanical Engineering
National Institute of Technology
Rourkela

STUDY OF SHEAR STRESS ON THE SURFACE OF AN OBSTACLE ATTACHED TO WALL OF A NARROW CHANNEL

A Thesis Submitted In Partial Fulfillment of the Requirements
For The Degree Of

Bachelor of Technology
in
Mechanical Engineering

Submitted by

Shivam Yadav
Roll Number – 111ME0352

Under the Guidance of

Dr. Amitesh Kumar

Department of Mechanical Engineering
National Institute of Technology
Rourkela

Department of Mechanical Engineering
National Institute of Technology, Rourkela

C E R T I F I C A T E

This is to certify that the work in this thesis titled ***STUDY OF SHEAR STRESS ON THE SURFACE OF AN OBSTACLE ATTACHED TO WALL OF A NARROW CHANNEL*** *by* ***Shivam Yadav (Roll – 111ME0352)*** *has been carried out completely under my supervision in partial fulfillment of the requirements for the degree of* ***Bachelor of Technology (B. Tech)*** *in* ***Mechanical Engineering*** *during session* ***2014 - 2015*** *in the* ***Department of Mechanical Engineering, National Institute of Technology, Rourkela****.*

To the best of my knowledge, this work has not been submitted previously to any other University or Institute or Organization for the award of any degree or diploma.

Dr. Amitesh Kumar
Assistant Professor
Department of Mechanical Engineering
National Institute of Technology Rourkela

A C K N O W L E D G E M E N T

I am extremely fortunate to be involved in this very exciting and challenging research project titled "***STUDY OF SHEAR STRESS ON THE SURFACE OF AN OBSTACLE ATTACHED TO WALL OF A NARROW CHANNEL***". It has enriched my life, giving me a golden opportunity to work in a new environment of Fluent. This project increased my thinking and understanding capability as I started the project from just a thought.

I would like to express my deepest gratitude and respect to my Supervisor ***Dr. AMITESH KUMAR***, for his constant and perfect guidance, valuable and thoughtful suggestions and of course endless support. His words of applause and sincere criticism throughout this year helped me a lot to develop my ideas regarding many important aspects of life. Not only that he has been an amazing supervisor but also a very genuine person. I consider myself extremely lucky to get an opportunity to work under his guidance. He is such a wonderful person my words will not be enough to express his grandeur.

I also extend my sincere thanks to all the faculty members of the Department of Mechanical Engineering for making my project successful, for their valuable advice in every stage and also giving me perfect working environment where I unleashed my potential.

At last, I would like to express my deepest sense of gratitude to GOD, and all those known and unknown hands which pushed me forward.

SHIVAM YADAV

111ME0352

D E C L A R A T I O N

I hereby declare that,

1. The work presented in this thesis is authentic and has been done completely by me under the general guidance of my supervisor.

2. The work has not been deposited to any other Institute/College/Organization for any degree/diploma courses.

3. I have followed all the Institute guidelines in writing the thesis.

4. Whenever I have used materials (data values, theoretical expressions and analysis, and texts) from any source, I have given them their due credit by citing them in the text of the thesis and providing details in the references.

SHIVAM YADAV

INDEX

LIST OF FIGURES

L I S T O F T A B L E S

A B S T R A C T

A numerical study has been carried out to determine the fluid shear stress variation on the surface of an obstacle placed in a narrow channel. In this 2D study the dimension of channel is taken as 100mm x 5mm and flow being laminar with Reynolds Number = 200 and velocity of fluid = 0.4m/s. The dimensions of the obstacle are varied to get 15 different shapes and then the variation of wall shear stress values on their surface obtained using ANSYS 15.0 software is studied. It is found that shear stress is minimum when the obstacle flatness is highest, and minimum when the obstacle flatness is least. Few other notable observations are reckoned. This study predicts that an obstacle caught in the flow will try to attain a shape as flat as possible, if it can change its geometry.

Keywords – narrow channel, micro channel, obstacle, shear stress variation, and flow past obstruction.

P R O J E C T O V E R V I E W

This study is divided into 3 chapters – INTRODUCTION, METHODOLOGY and RESULT & DISCUSSION. The details of the chapters are as detailed –

- Chapter : 1 – INTRODUCTION :

This chapter gives the details about this project work as how this idea was conceived, what importance it has, how much work is already done in this field and what I want to achieve through this project.

- Chapter : 2 – METHODOLOGY :

This chapter describes the method that has been used for this study and gives a brief introduction of how the things have proceeded towards the completion of this study.

- Chapter : 3 – RESULT & DISCUSSION :

This chapter is about the finding of this study and what are their causes and what conclusion can be drawn from them.

CHAPTER

1

I N T R O D U C T I O N

1.1 BACKGROUND –

In our daily life we see a lot of motions. Fluid flow being one of the most prominent among them. A fluid flows from a higher pressure region to a lower pressure region. While flowing, it very often comes across various objects which cause obstructions to its flow. Any obstruction in the path of flow leads to numerous phenomena. And because of this, flow past obstruction has been an area of intense research from a long time.

Various studies has been done in this field. Some include the flow characteristics after the obstruction while some discuss the effect that the obstruction causes in the flow. Some consider different geometry of obstacle while some consider different shapes. Some of them are as follows –

1. Supradeepan and Roy [1] performed Numerical simulations on two stationary circular cylinders placed side by side for a two-dimensional viscous incompressible flow at low Reynolds number (*Re*) 100. They varied centre to centre distance between the cylinders and solved the Navier – Stokes equations. For solving they used a finite volume method. Through this experiment they observed five different flow regimes.

2. Jiang and Lin [2] discussed about two tandem cylinders having different diameters. They considered two tandem cylinder of different diameter with fixed spacing and diameter ratio and performed a simulation based on the Lattice Boltzmann Method (LBM). They studied the effects of the width of channel and Reynolds number on the flow structures and force coefficients while changing the position of cylinders.

3. Wang et al. [3] studied flow around four cylinders which were placed in a square arrangement. They fixed the Reynolds number 8000. Then varied the pitch-to-diameter ratio between adjacent cylinders from P/D = 2 to 5 and changed the incidence angle from α=0 degree (in-line square configuration) to 45 degree (diamond configuration) at an interval of 7.5 degrees.

4. Lee and Yang [4] studied the flow patterns past two cylinders having equal diameter and arranging them in all possible configurations in terms of the distance between them and the angle of inclination of the line connecting the centre of cylinders with respect to the flow direction. They found that in all 10 flow regimes are possible.

Not only cylinders but other shapes like plates etc. are also studied.

1. Yoon and Jeong [5] investigated 2D stokes flow in a microchannel with a vertical plate as an obstruction. The force exerted and the drop in pressure induced by the obstructing vertical plate are calculated considering them as a function of blockage factor. They determined the drift velocity of the obstructing plate, for which the value of force exerted on the plate becomes zero and the then plate translates freely in the Poiseuille flow.

2. Seo and Kim [6] studied the micro mixer with various obstacles of various shapes. They calculated the concentration, flow and electric fields in the channel for various flow conditions.

3. Ozgoren et al. [7] experimentally investigated the flow characteristics around a sphere which is located over a smooth flat plate. They used dye visualization and PIV technique. They found that the ratio of gap has great influence on flow pattern of the wake and boundary layer interaction and the reattachment location variation of the separated flow from the surface of plate. Because of the effect of the boundary layer flow distribution the time-averaged flow patterns resulted into asymmetric structures downstream of sphere.

And not only in macro regions, a lot of work is also done in microchannel region –

1. Chang et al. [8] worked on a theoretical analysis for a novel microfluidic fuel cell which utilizes the laminar flows in a Y-shaped micro-channel to keep the separation between streams of fuel and oxidant without turbulent mixing.

2. Malboubi et al. [9] to understand the physical limits of cancer cell translocation in confined environments, they fabricated a microfluidic device to study ability of cancer cells to adapt their nuclear and cellular shape when passing through small gaps. They found that increasing cell confinement decreases their ability to translocate into small gaps and that cells cannot penetrate into the microchannel below a threshold cross section.

1.2 LITERATURE REVIEW –

Literature review aims at finding the work that has already been done in the concerning field. Following are some of the many work done in the concerning field –

Hammer and Apte [10] described a numerical method which simulates the interaction between a single cell and a ligand-coated surface that is under flow. They idealized the cell as a microvilli-coated hard sphere that is covered with adhesive springs. At each time step the velocity of cell in the simulation resulted from a balance between hydrodynamic, colloidal and bonding forces. With their model the effect of many parameters on adhesion can be simulated some of them being number of receptors on the tip of microvilli , ligand density, reaction rates between receptor and ligand, the stiffness of resulting ligand- receptor springs, springs responses towards strain, and bulk hydrodynamic stress magnitude. Also, their method can generate some meaningful statistical measures of adhesion, such as the mean and variance in velocity, rate constants for cell attachment and detachment, and adhesion frequency.

Tissot et al. [11] described an experimental study done on both the translational and rotational velocities of the leukocytes sedimenting on a flat surface under the laminar shear flow. They concluded that (a) Cells move with constant velocity close to the wall for several tens of seconds. (b) The velocity values (translational and rotational) are not consistent with the Goldman's model for a neutral buoyant sphere in a laminar shear flow, unless a drag force is added that corresponds to the contact friction between the cells and the floor of the chamber. (c) It was also shown that the higher value of the cell-to-substrate gap can be accounted for by the presence of cell surface protrusions which are of a few micrometer length, (d) the results were consistent with the possibility of cell-substrate attachment which is initiated by the formation of a single molecular bond, which can be taken as the rate limiting step.

The dynamic interplay between local hemo-dynamic milieu, low Endothelial Shear Stress (ESS) in particular, and wall biology can be very important in the atherosclerotic wall remodeling. Chatzizisis et al. [12] explored the processes supporting the role of low endothelial shear stress in the natural history of coronary atherosclerosis and vascular remodeling at the molecular, cellular, and vascular level. This indicated similar mechanisms regarding different natural historical trajectories of any individual coronary lesions. Atherosclerotic plaques that were associated with excessively expansive remodeling evolved to high-risk plaques, because of the persistence of low ESS conditions, and thereby promoting continued local accumulation of lipid, inflammation, oxidative stress, breakdown of matrix, and finally further more plaque progression and excessive expansive remodeling.

Gavze and Shapiro [13] showed that the wall effects decrease with the increasing particle non-spherisity (that is reducing aspect ratio). For particles that are long and slender the effective distance where the wall effect is significant can be measured using several particle shorter axes. In the wall vicinity region spheroids experience a number of interactions, which however do not exist in case of spheres. The study also revealed that the effect of the wall is to cause creation of a nonzero velocity component in the direction of the normal to the wall surface. This velocity is nil in case of a spheroids in free shear flow; and near the wall it vanishes for spherical and, seemingly, for oblong particles. Thus in a shear flow a spheroid moving near the wall will perform an oscillatory motion which is in towards and away directions from the wall.

Sabiri et al. [14] in their experiment measured the local shear rate on the surface of a cylinder which was exposed to a fully developed laminar flow of power-law fluids in a vertical pipe using the platinum made Micro-electrodes. They found that the shear rate value is at maximum when $\Theta = 130^{\circ}$ and it tends to be greater in case of shear-thinning fluids compared to the case of Newtonian fluids.

Furukawa et al. [15] developed a new system to evaluate the detachment force of cells with utter ease. Their system was developed on a modified cone and plate-type viscometer which was equipped with an epi-fluorescence microscope in upright condition. Just a small volume of medium, cells, and a small material piece were enough to evaluate the cell detachment by shear stress.

Gaver and Kute [16] predicted the amplification of mechanical force, stress, and torque on an adherent cell arising from a flow within a narrow microchannel. They modelled the system as a bulge of semicircular shape on a microchannel wall, with a pressure-driven flow. They used algebraic expressions derived from lubrication theory which can be used accurately with utter simplicity to predict the force, fluid stress, and torque based upon the viscosity of fluid-μ, height of channel-H, size of cell-R, and flow rate per unit width, $Q_{2\text{-d}}$. The study showed that even for the very small cells ($\gamma = R/H \leq 1$), the force, stress, and torque can be quite greater than that predicted for a flow in a cell-free system. Elevated resistance to flow and higher fluid stress amplification occur with cells of bigger size ($\gamma > 0.25$), because of constraints caused by the channel wall.

Williams et al. [17] evaluated of interfacial stresses with a standard, finite-difference based, immersed boundary method. They investigated 3 model flow problems at very low values of Reynolds numbers. Then compared the results obtained from the immersed boundary method to those achieved by the boundary-element method (BEM). The stress on an immersed boundary can be calculated either by direct evaluation of the fluid-stress (FS) tensor or, for the stress jump, by direct evaluation of the locally distributed boundary force (wall-stress or WS). Through their

study they concluded that the immersed boundary method can provide quite reliable approximations to interfacial stresses.

Hazel and Pedley [18] calculated the distribution of forces exerted on a 3-D hump, (that represents the raised cell nucleus), by a uniform shear flow. For a non-axis-symmetric ellipsoidal hump, it is found that, the least total force is exerted when the hump is in line with the flow. Furthermore, for a hump of fixed volume, there exists a specific aspect ratio combination for which the total force upon the hump is least, (0.38:2.2:1.0; height : length : width). This combination is approximately the same as the average aspect ratio taken up by the cell nuclei in vivo (0.27:2.23:1.0). Therefore, it is possible, that the cells respond to the flow in such a manner that the total force on their nuclei is minimum.

1.3 MOTIVATION –

Fluid dynamical stresses possess great importance in the regulation of many physiological phenomena, such as the growth of athero-scolatic plaque in small veins occurs in the presence of a low and oscillatory wall shear stress. Another good example is the functioning of epithelial cells, which are found in the lining of the pulmonary airways – here potentially damaging normal and shear stresses can arise during reopening of airways when artificial ventilation of premature neonates takes place. The response of cells to the mechanical stresses is an important factor in many biological processes for example – cell-division, embryo-genesis, cell-migration diapedesis etc. Typical examples concern the reaction to shear stresses exerted as cells travel through the blood or when they adhere to vascular wall, but also within tissues because cells are exposed to various forces due to its environment.

To a simple generalization cells exert a different response as a function of substrate stiffness and develop stronger forces when the substrate is more rigid. They also develop larger forces as a function of its environmental conditions resulting in cell polarization, however their orientation may also depend upon the type of forces they are acted upon like static, quasi-static or periodic stresses.

Cells very often adhere to the walls of the channels/tubes if their cross-sectional dimensions match to those of the cells themselves. This adhesion of cells to walls can occur in situations which are as varied as leukocyte adhesion to the microchannel wall. Reaction to mechanical stresses involve mechano-transduction or how the forces are converted in biological and functional response.

To fully understand the inter-relationship between cell behavior and flow, a fundamental understanding of the modification of the flow field within channel, the flow induced shear stresses, force and torque on body of the cell is necessary. Various different lines of research can be benefitted from the better understanding of the hydro-dynamic interaction between a cell and its environment. Leukocyte adhesion, biofilm production to name a few.

1.4 OBJECTIVE –

As we have seen that the shear stress on the surface of obstacle is of utmost importance. It dictates so many phenomena in micro channel. Not only phenomena many processes occur because of these shear stress only. However in the case of macro-channels the role of shear stress is not so pronounced because the region where impact of the shear stress is felt is comparatively smaller than compared to the dimensions of channel.

But in small channels called as mini channels or narrow channel there effects can be pronounced.

Thus in this study we take up narrow channel as our zone of interest.

Our aim is to "STUDY OF SHEAR STRESS ON SURFACE OF AN OBSTACLE ATTACHED TO THE WALL OF A NARROW CHANNEL USING CFD".

In this work it is planned to find the values and variation of shear stress on obstacle surfaces of various shapes for example circle, ellipse and then perform an in depth study.

CHAPTER

2

METHODOLOGY

2.1 COMPUTATIONAL FLUID DYNAMICS (CFD) –

Computational Fluid Dynamics is a branch of fluid mechanics that uses numerical methods and various algorithms to resolve and analyze problems that involve the fluid flows. Computers are used to perform huge calculations needed to simulate the interaction of fluids with the intricate surfaces. Though very accurate sometimes even with basic equations and high-speed supercomputers, only approximate solutions can be reached. Through various research, however, we may produce a software that advances the correctness and speed of intricate simulation conditions like turbulent flows. Initial verification of any such software is performed using a wind tunnel but the final validation comes from flight test. The most vital job performed by the computer in CFD is to treat a continuous fluid in a discretized way. One simple technique to do this job is to discretize the 3-D domain into number of small cells to generate a volume grid or mesh, and then applying an appropriate algorithm to solve the equations of motion. Also this meshing can be either irregular or regular. If we choose however not to pursue a mesh-based technique, there are a number of substitutes, notably Smoothed Particle Hydrodynamics, Spectral methods and Chebyshev polynomials. When all of the applicable length scales can be determined by the grid then we can directly solve the problems involving laminar and/or turbulent flows easily by Navier- Stokes equations.

2.1.1 DISCRETIZATION METHODS IN CFD –

The steadiness of the discretization method is generally known numerically than analytically as in case of simple linear problems. We must make sure that the discretization is taking care of discontinuous solutions elegantly. These are some of the discretization methods that are generally used in CFD–

a) Finite volume method (FVM):

FVM takes the PDE's (Partial Differential Equations) of the N-S equation in the traditional form then discretizes it. This method promises the conservation of fluxes through a specific control volume. In this method there is no assurance that the solution is definite even when the general explanation is conventional. Furthermore FVM is subtle to distorted elements which can avoid convergence if these elements are present in flow regions which are critical for the study. This integration method thus produces a method that is integrally conventional.

b) Finite element method (FEM):

This method is generally used for structural analysis of solids, but is also appropriate for fluids. For use with the N-S equations the FEM designs have been modified. It is quite steadier than the

FVM, even though in FEM conservation needs to be taken care of. Normally robustness of the solution is better in FEM however in some cases it might take higher recollection than FVM.

c) Finite difference method (FDM):

This technique is very old and is very simple to program. These days' finite difference codes make use of an embedded boundary for treating complex geometries which makes these codes highly effective and precise. In FDM the solution is interpolated across each grid but there are other ways to handle geometries that are using overlapping-grids. The boundary employed by the fluid in this method is divided into surface mesh.

2.1.2 HOW DOES CFD WORK?

The development of high performance affordable computing hardware and the availability of user-friendly interfaces have led to the development of commercial CFD packages. Before these CFD packages came into the ordinary use, one had to write his own code to carry out a CFD analysis. The programs were usually different for different problems, although some part of the code of one program could be used in another. The programs were inadequately tested and reliability of the results was often questioned. Today, well tested and established commercial CFD packages not only have made CFD analysis a routine design tool in industry, but are also helping the research engineer in focusing on the physical system more effectively.

Hence all CFD packages comprise of three key elements:

1. Pre-processing.

2. Solver

3. Post - processing.

a) PRE-PROCESSING:

Pre-processor consists input of the flow problem with the help of an easy interface. This input is converted into suitable form for use by the solver. The actions to be performed by the user at the Pre-processing phase include:

1) Description of the geometry of the region: The domain where the computation is to be done. Grid generation is the next step which includes subdivision of the domain into a number of lesser or no overlapping sub domains.

2) Explanation of fluid properties: The solution to a flow problem is performed at nodes inside each cell the description of suitable boundary conditions at cells that is coincident with the boundary. The number of the cells in the grid governs the correctness of the CFD solution. Usually, the larger numbers of cells better the solution correctness. Both the accuracy of the solution & its cost in terms of essential computer hardware & calculation time are dependent on the fineness of the grid.

b) SOLVER:

The solver is the heart of CFD software. It sets up the equations which are selected according to the options chosen by the analyst and grid points generated by the pre-processor, and solves them to compute the flow field. The process incorporate the following tasks:

- defining appropriate physical model,
- defining material properties,
- providing boundary conditions,
- generating initial solution
- defining solver controls
- defining convergence criteria,
- solving the set of equations,
- generating the results

Once the model is completely set, the solution is initialized consequently calculation starts and intermediate results can be monitored at every time step from iteration to iteration. The progress of the solution process get displayed on the screen in terms of the residuals, a measure of the extent to which the governing equations are not satisfied

c) POST-PROCESSING:

In the post-processing huge amount of development work has newly taken place. Due to the ever increased acceptance of engineering work stations, many of which has excellent graphics abilities, CFD packages are now equipped with multipurpose tools for data visualization. These include –

1) Domain geometry & Grid display

2) Vector plots

3) Line & shaded contour plots

4) 2D & 3D surface plots

5) Particle tracking

6) View manipulation (translation, rotation, scaling etc.)

2.1.3 OVERVIEW OF FLUENT PACKAGE –

FLUENT is a state-of-the-art computer program used for modeling of problems involving heat transfer and fluid associated with complex geometry. FLUENT provides complete mesh flexibility, solving one's flow problems with unstructured grids that can be generated about complex geometries with relative ease. Supported grid types include 2D triangular/quadrilateral. 3D FLUENT also allows user to refine or coarsen grid based on the flow solution.

FLUENT is written in C programming language and it fully uses of the flexibility and power offered by C language. Because of this there are a lot of benefits {like true dynamic memory allocation, efficient data structures, and flexible solver control (user defined functions)}. In addition, FLUENT uses a client/server architecture, which allows it to run separate simultaneous processes on client desktop workstations and powerful computer servers, for efficient execution, interactive control, and complete flexibility of machine or operating system type.

All functions necessary to compute a solution and display the results are accessible in FLUENT through an interactive, menu-driven interface. The user interface is written in a language called Scheme, a dialect of LISP. The advanced user can customize and enhance the interface by writing menu macros and functions

2.1.4 CFD PROCEDURE –

For numerical analysis in CFD, it requires five stages such as:

- Geometry creation
- Grid generation
- Flow specification
- Calculation and numerical solution
- Results

Based on control volume method, 3-D analysis of fluid flow and heat transfer for the helical coiled tube has been done on ANSYS FLUENT 15.0 software. All the above mentioned processes are done using the three CFD tools which are pre-processor, solver and post-processor.

Figure 1 gives a general idea of how the things are done on the ANSYS. The preprocessing includes creation of desired geometry and the creating a mesh of it. Mesh is basically the discretization of the whole geometry. During meshing the whole geometry is divided into small grids on which the various conditions are applied and the numerous equations are solved in Solver module. During the post processing data is extracted from the solution generated by the solver. This data extraction can be done is various ways – we can get a graph of it or a contour diagram of it, it can also create a representation of the vector quantities or we can directly extract values and use them as per our wish and need.

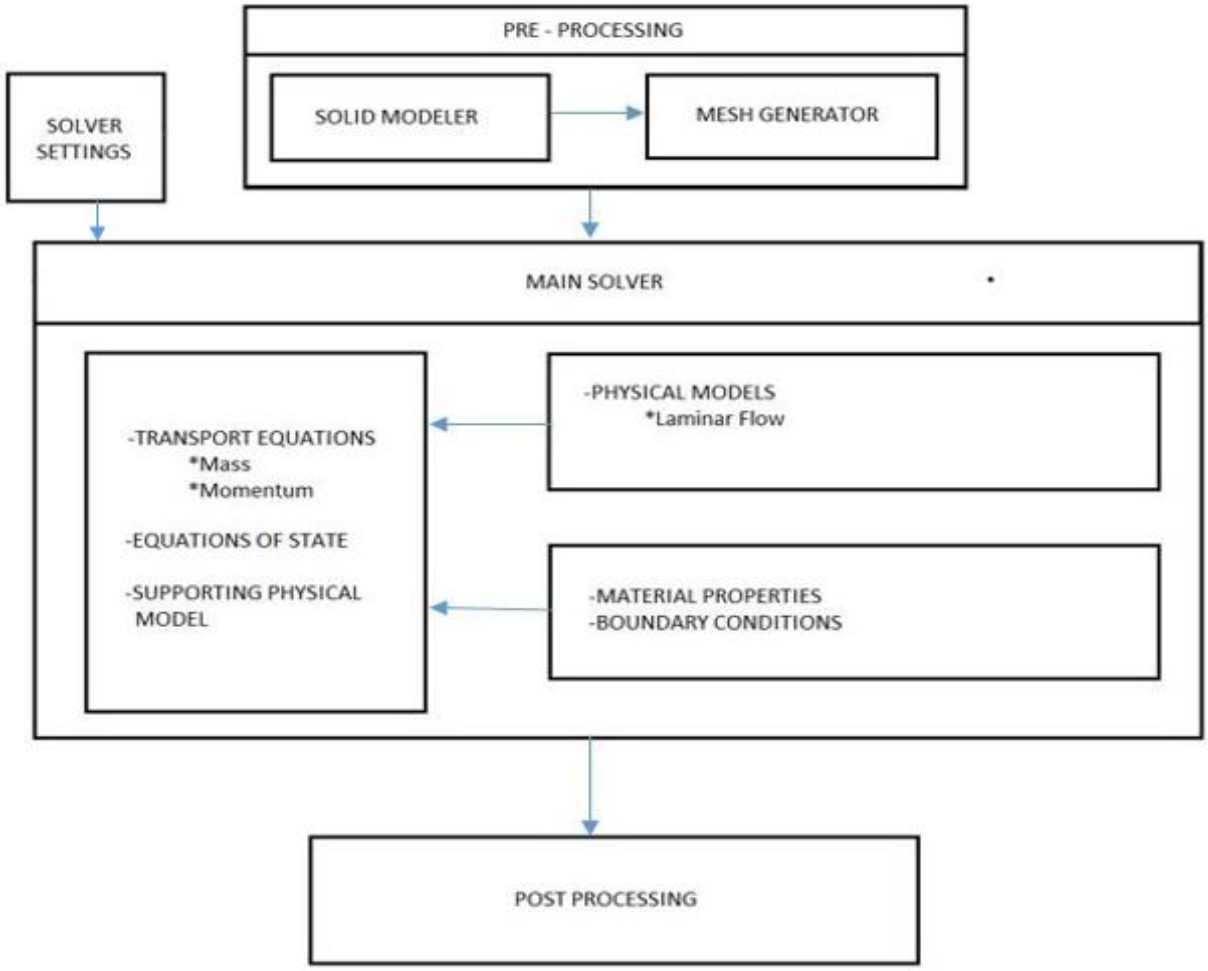

FIG 1 - OVERVIEW OF MODELLING PROCESS

2.1.5 DETAILS OF PRESENT STUDY –

In this study a channel of 100mm x 5mm dimension is taken.

Then an obstacle is created on the bottom surface of the channel. And the dimension of this obstacle is varied from to get 15 different shapes. The obstacle is taken of half of elliptical shape (ellipse shape divided into 2 parts by the semi major axis) with semi major axis (b) taking values 1mm, 1.5mm, 2mm and the semi minor axis (a) taking values 0.2mm, 0.4mm, 0.6mm, 0.8mm, 1mm. In this variation a special case is generated when a = b = 1 mm i.e. formation of a semicircle.

Then for these different cases variation of shear stress is calculated using the ANSYS FLUENT 15.0.

2.1.6 GEOMETRY CREATION –

The geometry creation in ANSYS 15.0 is done in 'Design Modeler'. It is a simple application with easy to follow and understand UI. Design modeler allows us to create 2D or 3D geometries depending upon our interest.

This being a 2D study of a channel becomes quite simple to design.

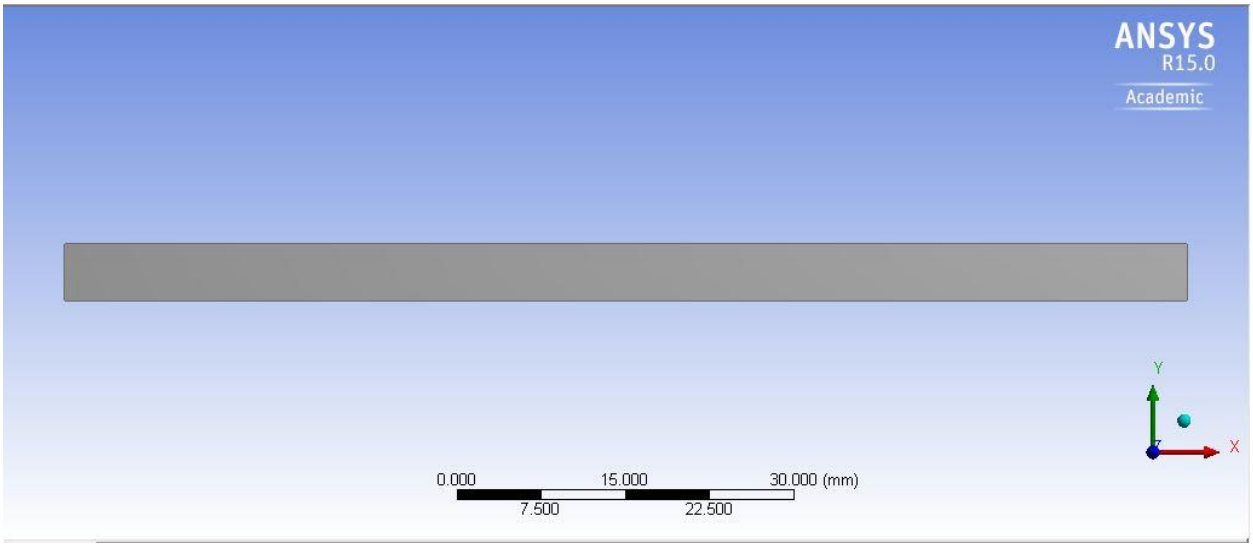

FIG 2 – Geometry for flat channel study

FIG 2 shows the geometry of channel designed for the study of fluid shear for flat channel that doesn't have any obstacle attached to it. The length of the channel is taken 100mm while the breadth of the channel is taken as 5mm.

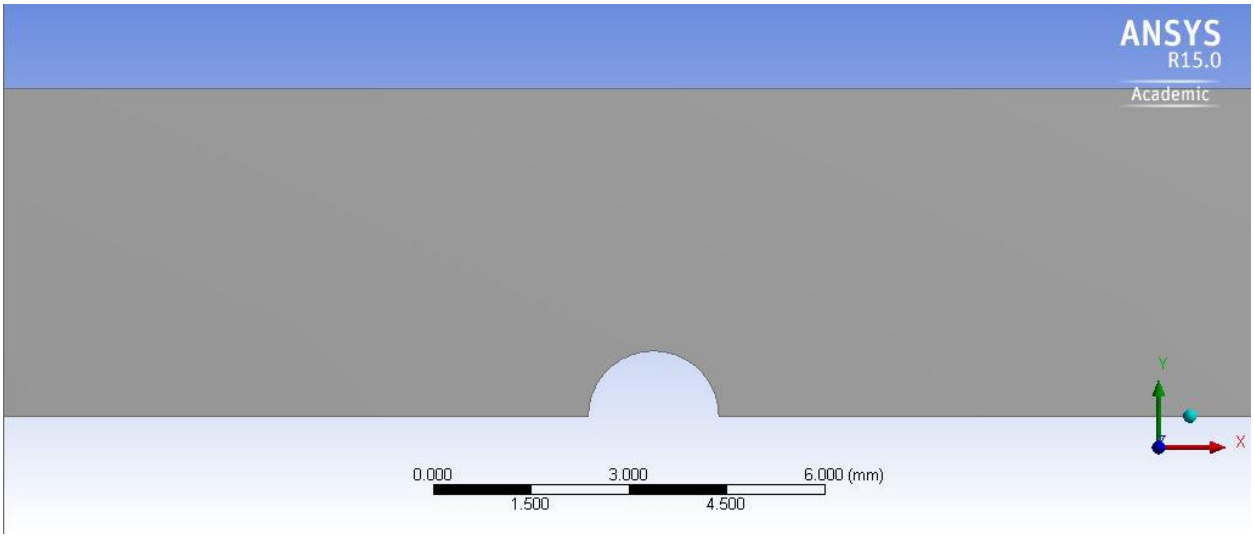

FIG 3 – Obstacle geometry for case 13 i.e. when ‘a’=1mm and ‘b’=1mm

Figure 3 gives a zoomed view of the channel with an obstacle having ‘a’ = 1mm and ‘b’ = 1mm. The distance between the inlet edge and the center of obstacle is taken as 55mm the reason behind 55mm being that the flow is fully developed in that region and we are interested in fully developed region only.

Table 1 – Various geometries of obstacle

CASE NUMBER	‘a’ = Semi Minor Axis in mm	‘b’ = Semi Major Axis in mm
1	0.2	1
2	0.2	1.5
3	0.2	2
4	0.4	1
5	0.4	1.5
6	0.4	2
7	0.6	1
8	0.6	1.5
9	0.6	2
10	0.8	1
11	0.8	1.5
12	0.8	2
13	1	1
14	1	1.5
15	1	2

Table 1 shows the various geometries of the obstacle that are studied in this work. They will hence forward be referred by their case number.

2.1.7 MESH GENERATION –

In mesh generation the geometry of the object or region under study is divided into a grid of small size cells on which various calculations are performed in solver.

Figure 4 shows the meshing done for the study of flat channel. The whole channel was divided into 1000 x 50 i.e. 50000 cells. As a thumb rule we can say that finer the grid i.e. larger the number of cells the better the solution is. But after a certain cell size the solution does not change much on increasing the grid size or reducing the size of cell. This is why we need to perform a grid independence test to find the optimum size of the cell.

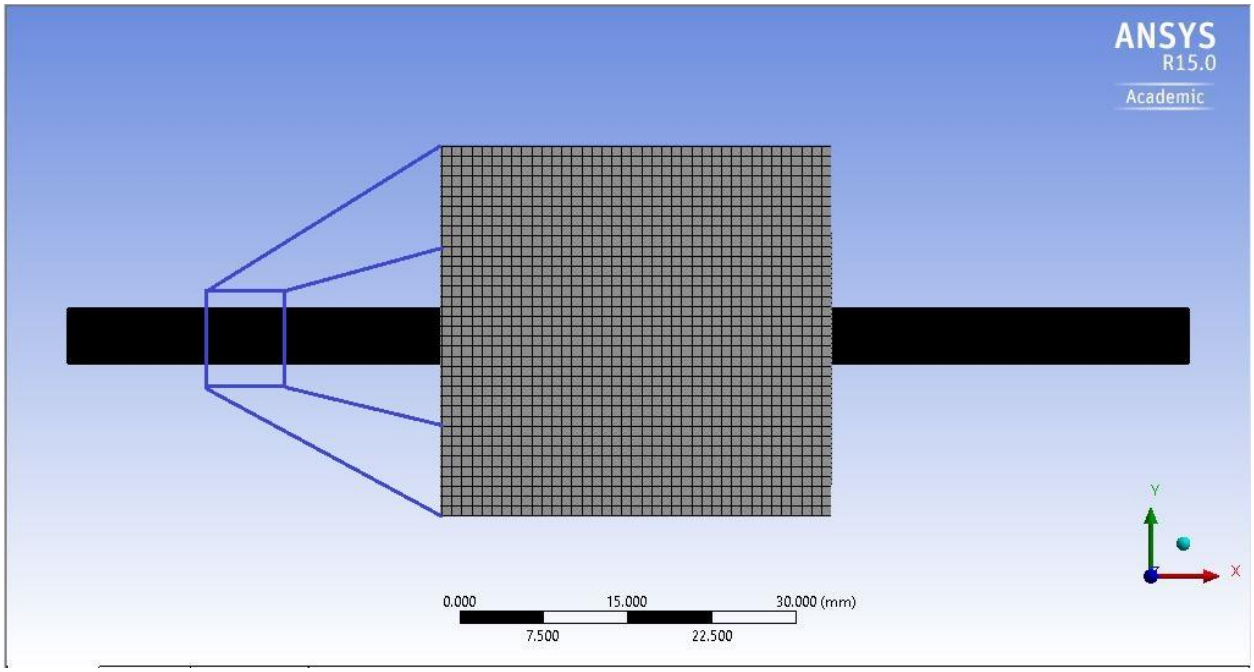

FIG 4 – Meshing for flat channel the box shows the zoomed meshing area

For the flat channel when grid independence test is done it is found that 1000x50 grid size gives good results which do not vary much on increasing the size of grid (further lowering the size of unit cell). The following graph shows that on increasing the grid size (or lowering the size of unit cell) the change is values of wall shear is of the order of 0.2%. Thus 1000x50 grid size is taken for the analysis as it gives satisfactory results without causing huge the no of iterations for the solution to converge.

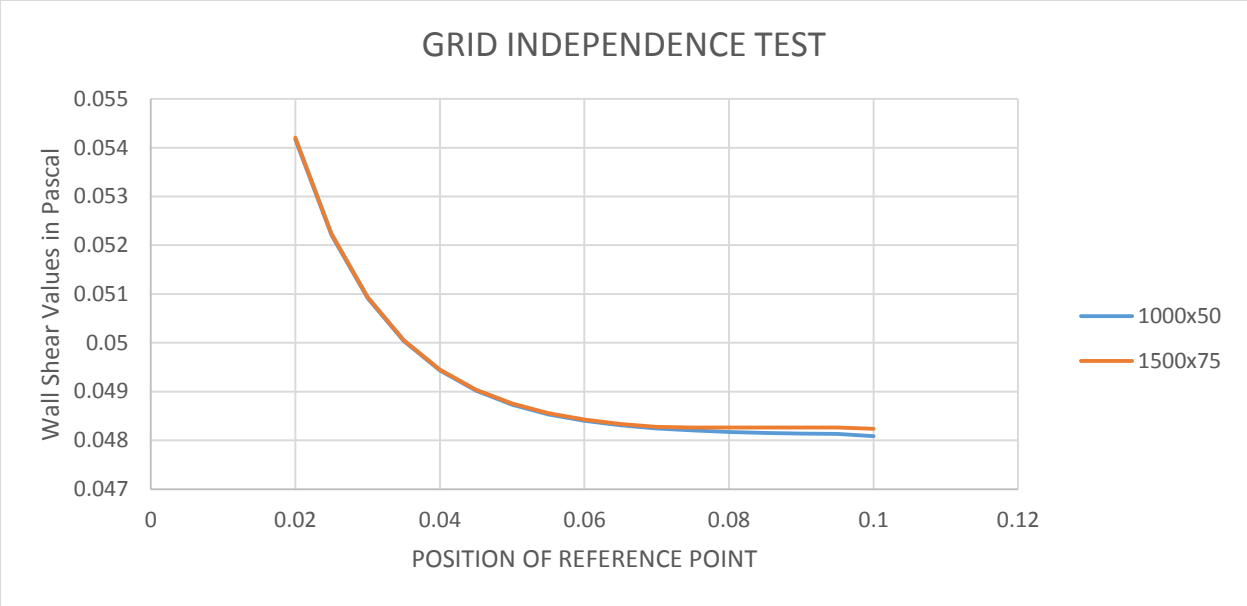

FIG 5 – Grid independence test on flat channel

The following figure (fig 6) shows the meshing for the 13th case of obstacle in the bottom of the channel. In this 13th case 'a' = semi-minor axis = 1mm and 'b' = semi-major axis = 1mm. Since the meshing is very fine this figure does not properly show the meshing done. Thus in the next figure (fig 7) a zoomed view of the meshing region marked by a box in fig 6 is shown.

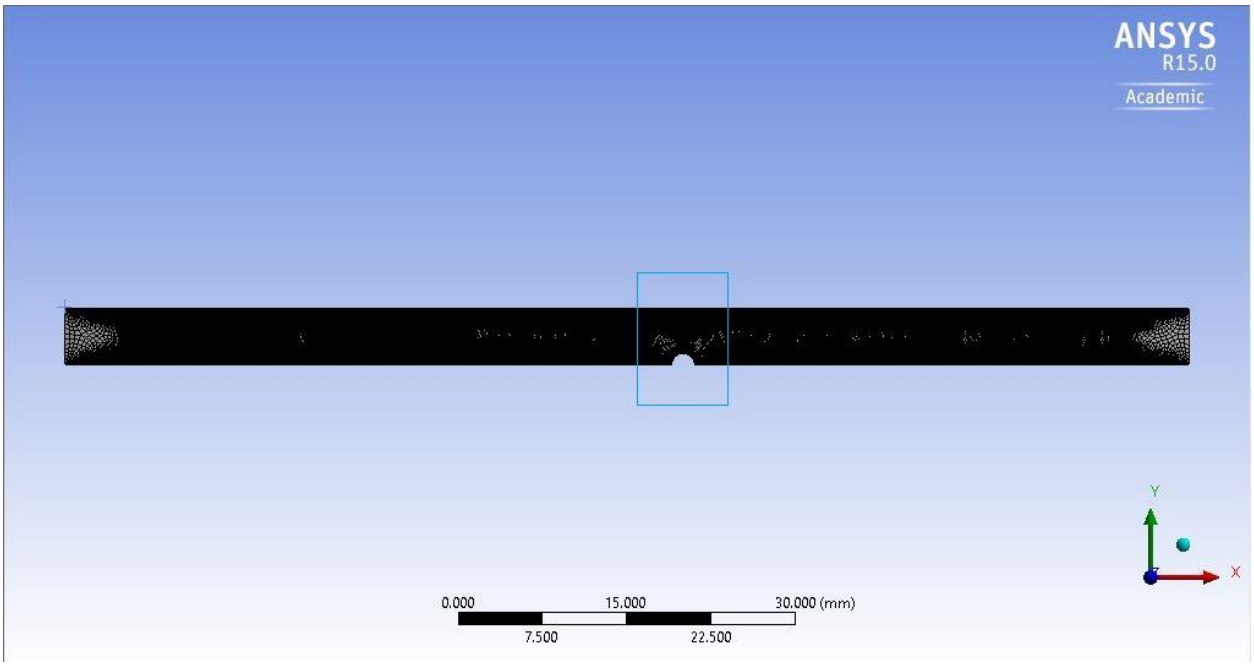

FIG 6 – Meshing for case 13 i.e. when 'a'=1mm and 'b'=1mm

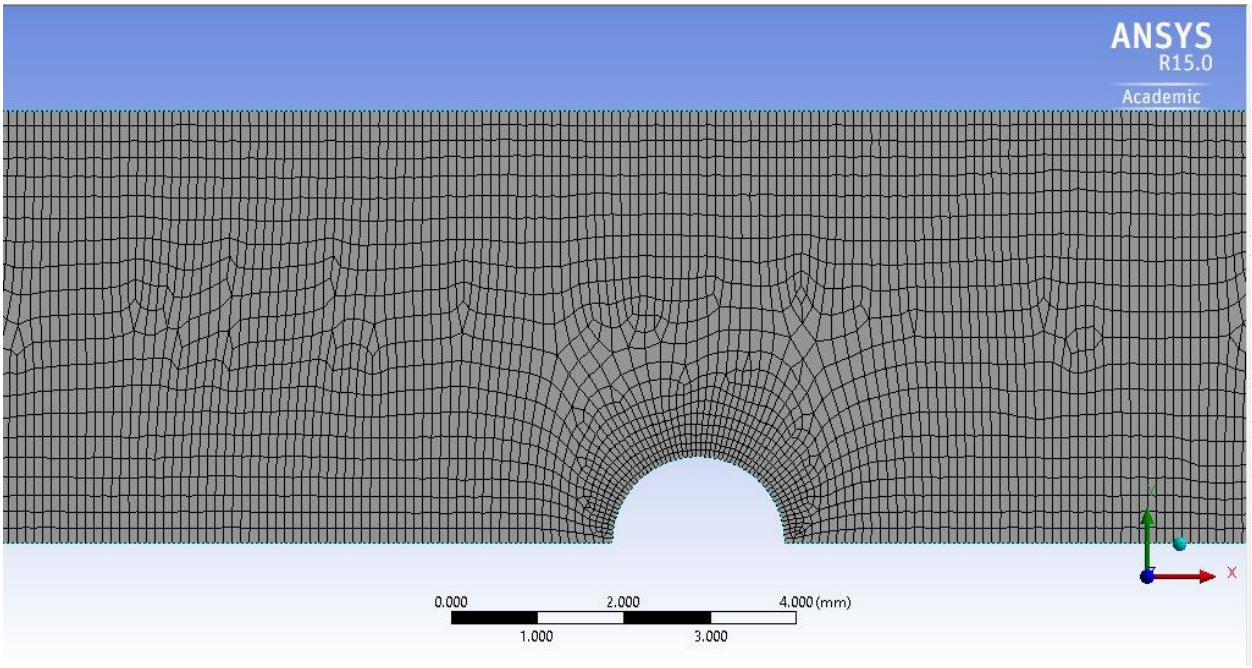

FIG 7 – Zoomed view of meshing for case 13 i.e. when ‘a’=1mm and ‘b’=1mm

2.1.8 FLOW SPECIFICATION –

The assumptions used in this model were

a. The flow was steady and incompressible.

b. Water is taken as the flowing fluid (with its density, viscosity, specific heat and other values being constant).

For the present analysis the method applied is explained below. All the governing equations used in present analysis were solved by using ANSYS FLUENT 15.0 finite volume commercial code. Second order upwind scheme was used for solving momentum. The convergence criterion was fixed such that the residual value was lower than 1e-6. The pressure correction approach using the SIMPLE algorithm was used.

Table 2 – Relaxation factor			
Pressure	Momentum	Density	Body Force
0.3	0.7	1	1

Relaxation factor have been kept to default values and shown in table 2.

TABLE 3 – BONDARY CONDITIONS		
Inlet	Velocity inlet	Velocity = 0.04 m/s
Outlet	Pressure outlet	Gauge Pressure = 0
Top	Stationary wall	No slip condition
Bottom	Stationary wall	No slip condition
Obstacle	Stationary wall	No slip condition

The table 3 gives the details of the boundary conditions applied to the various elements of the geometry.

The inlet velocity value is decided as 0.04m/s so that the value of Reynolds number is 200.

CHAPTER

3

RESULT AND DISCUSSION

3.1 FOR FLAT CHANNEL –

First of all to check the validity of the method being used to find the shear stress values, we applied the method on a flat channel with no obstacle.

From the study of viscous flow between two parallel flat plates we know that the maximum value of shear stress occurs on the surface of flat plate itself. And the value of this shear stress is given as $\tau = -\frac{1}{2}\frac{\partial p}{\partial x}t$

Where

τ refers to the shear stress value at plate surface.

$\frac{\partial p}{\partial x}$ Refers to the variation of pressure along the x-direction (this value is constant along y-direction)

t refers to distance between the plates which is 5mm = 0.005m.

We obtained the values of total pressure at plate surface along the x-direction at an interval of 0.1mm. 0.1 mm being quite small in comparison to 100mm length of the channel we evaluated the

$\frac{\partial p}{\partial x}$ As $(p_{i+1} - p_i) / (x_{i+1} - x_i)$

Multiplying the obtained values with (-0.5) and (0.005) we get the values of shear stress.

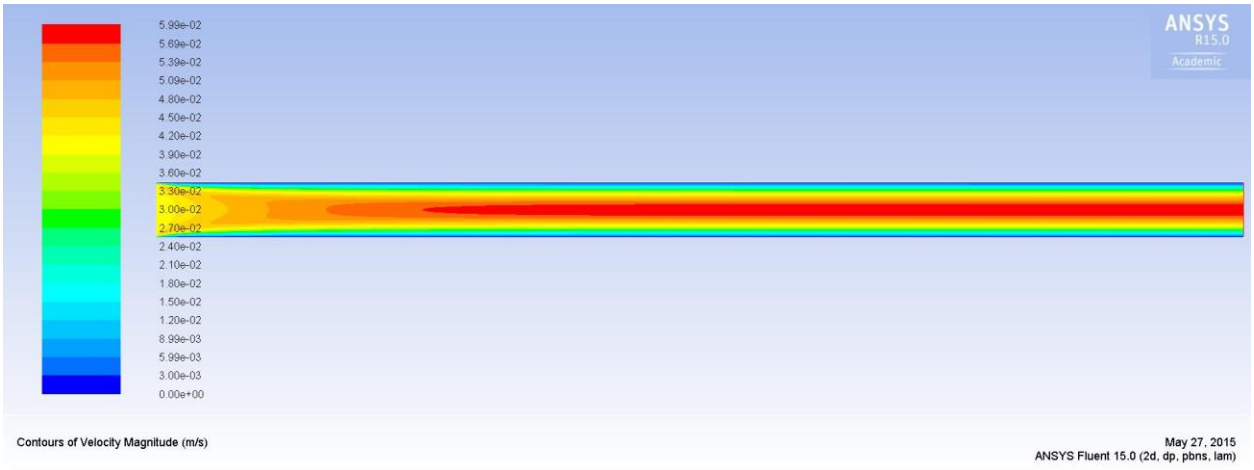

FIG 8 – Velocity contour for flat channel

From the velocity contour diagram (8) for a flat channel we can observe that a region of high velocity (shown in reddish orange color) forms in the middle of channel that does not change along the length of the channel. The point from where region starts marks the beginning of the fully developed zone. Before that region the flow is developing and velocity changes along the length as well as breadth of the channel, we are not interested in this region of the flow. We are interested only in the fully developed region.

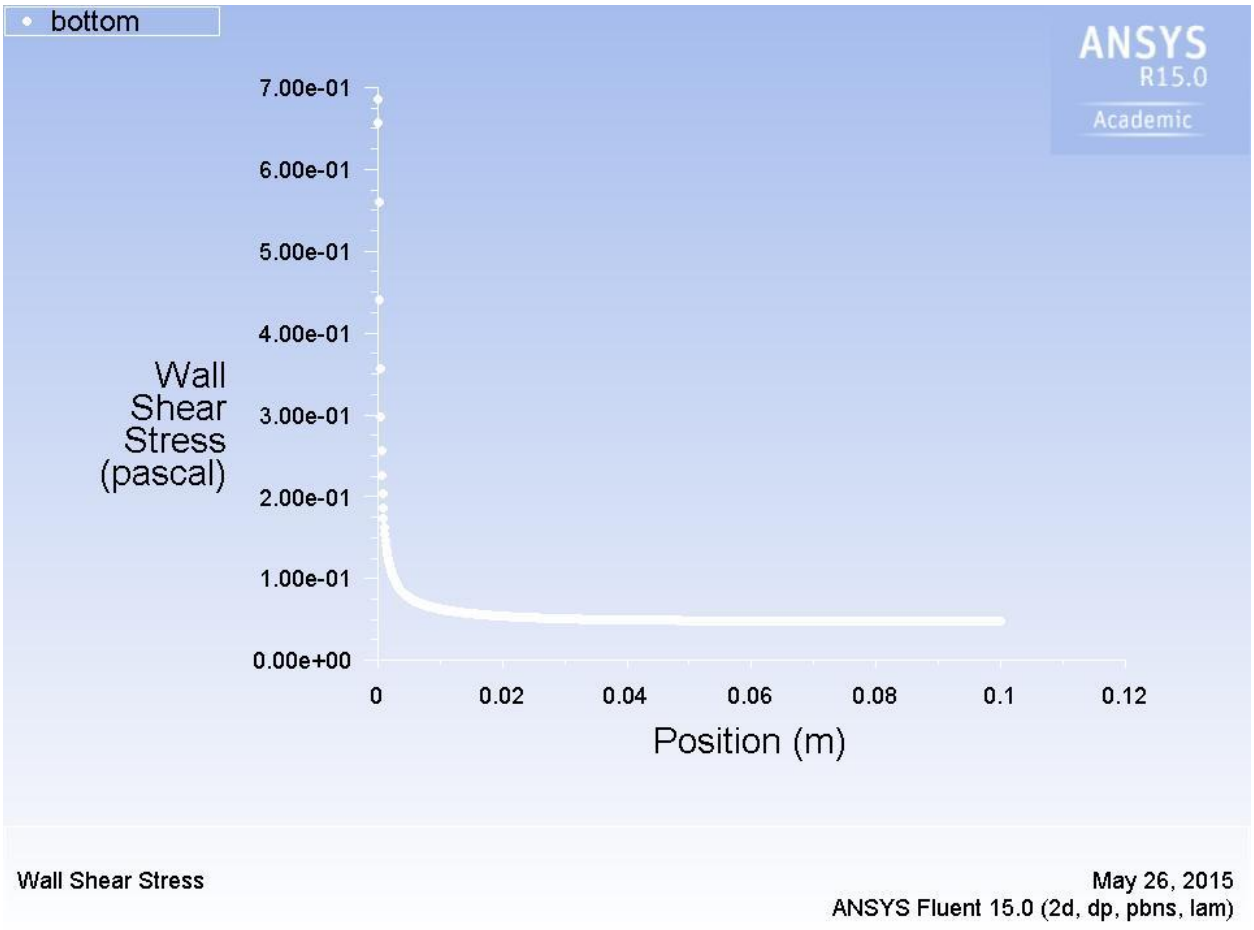

FIG 9 – Variation of wall shear along the length of the channel.

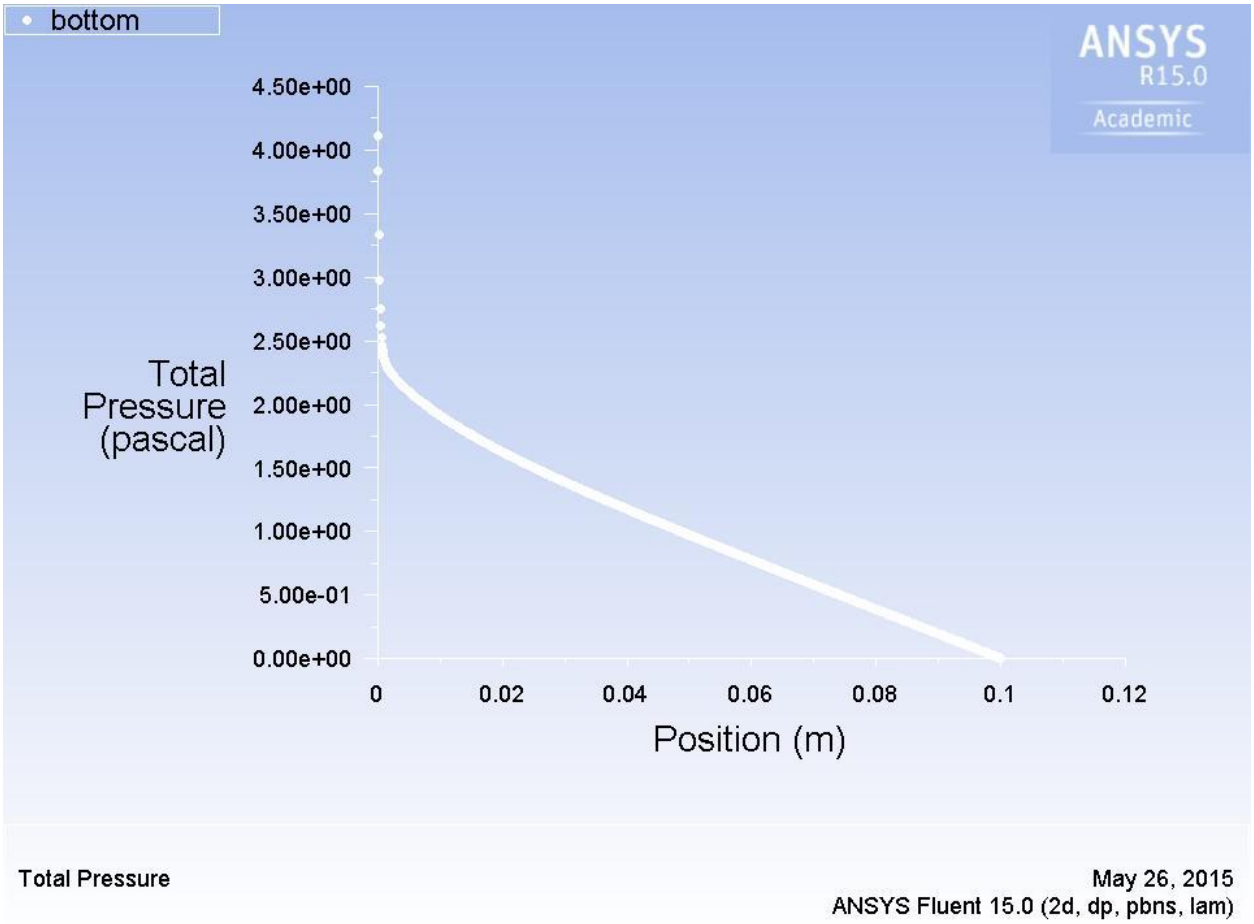

FIG 10 – Variation of total pressure along the length of channel.

From the graph in FIG 9 we observe that in the starting when the flow is developing the value of shear stress is very high but after as the flow develops the value of wall shear comes down drastically and the becomes constant when the flow is fully developed.

This is justified from the theory given that value of wall shear depends on the pressure variation along the length of the channel and from the variation of total pressure we can observe that in the developed region the $\frac{\partial p}{\partial x}$ becomes constant as shown in FIG 10 and thus no change in value of wall shear.

The FIG 11 shows the percentage error between the values of wall shear obtained directly through CFD and those obtained using the theoretical formula. The maximum error is of about 2.24% which can be accepted as being in admissible range. This also validates the method being used to find the variation of shear stress.

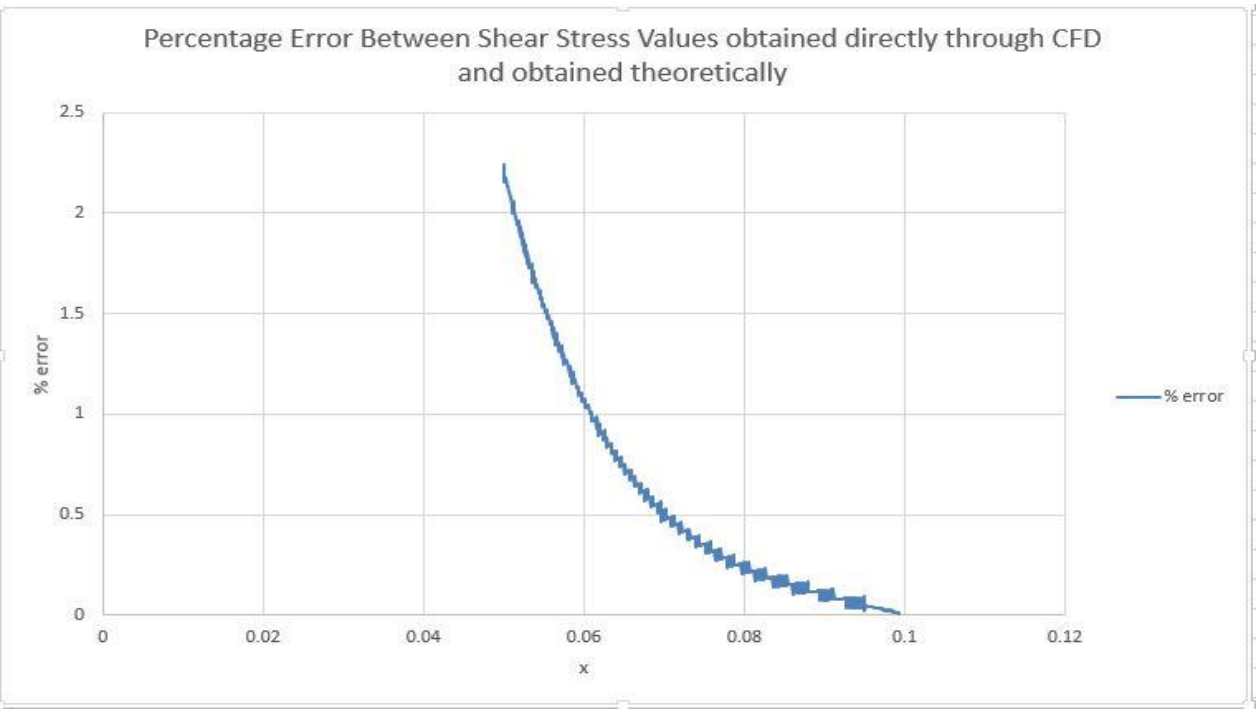

FIG 11 – The percentage error variation between the values of wall shear obtained directly through CFD and those obtained using the theoretical model.

3.2 CHANNEL WITH OBSTACLE –

We then perform the same procedure with the channel having obstacle as we did in the case of flat channel.

3.2.1 Velocity Profile –

The basic reason behind the existence of fluid shear stress is viscosity of fluid. The viscosity of the fluid is the resistance offered by a fluid layer to the next adjoining fluid layer when they move with different velocity. Thus studying the velocity profile is very important.

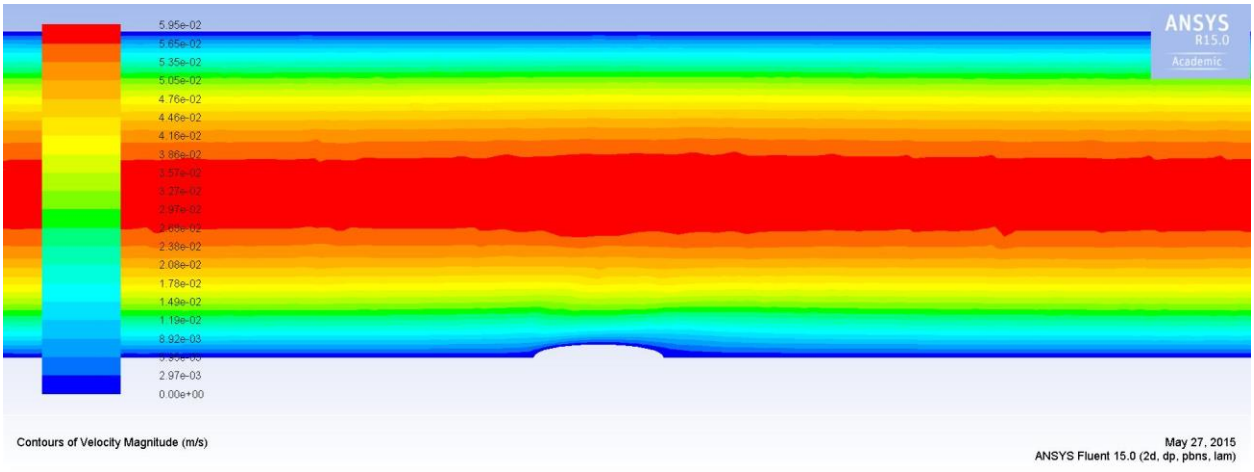

FIG 12 – Velocity contours for case 1 i.e. ‘a’ = 0.2mm & ‘b’ = 1mm.

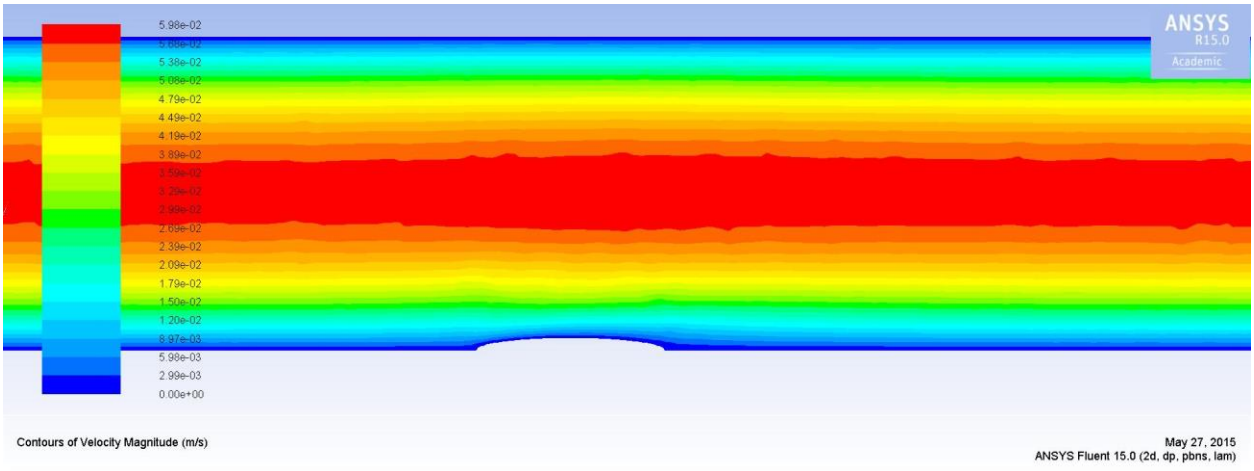

FIG 13 – Velocity contours for case 2 i.e. ‘a’ = 0.2mm & ‘b’ = 1.5mm.

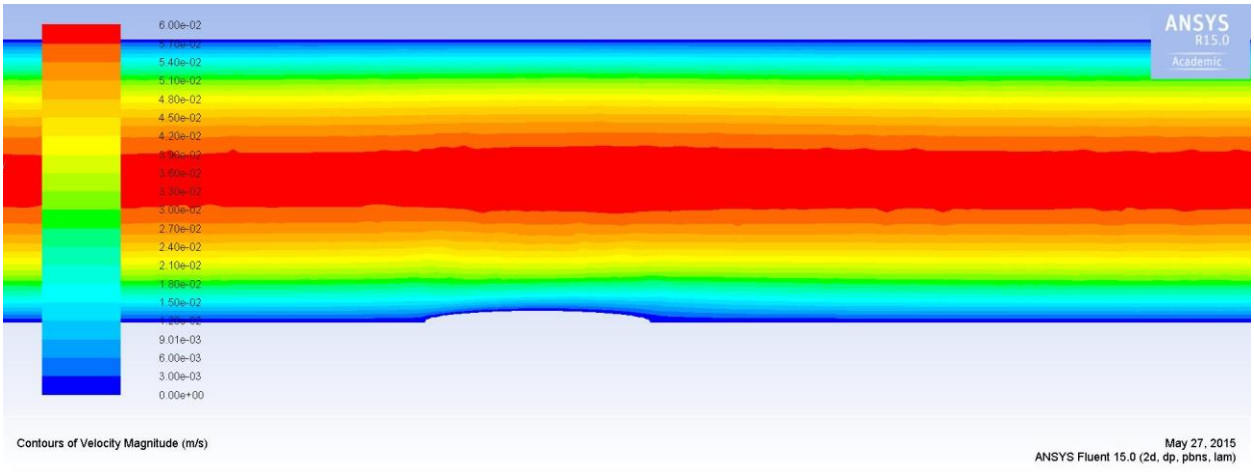

FIG 14 – Velocity contours for case 3 i.e. ‘a’ = 0.2mm & ‘b’ = 2mm.

FIG 12, 13, 14 represent the velocity contours for the case when the longitudinal height is the least of all cases ‘a’ = 0.2 mm and latitudinal length ‘b’ = 1mm, 1.5mm, 2mm respectively. As we can clearly observe from the velocity contour diagram that in the case 3 the contours are most similar to that of flat channel without any obstacle. This arises from the geometry of the obstacle as in 3rd case the surface profile of obstacle is very elongated and without much height to produce any change in contour.

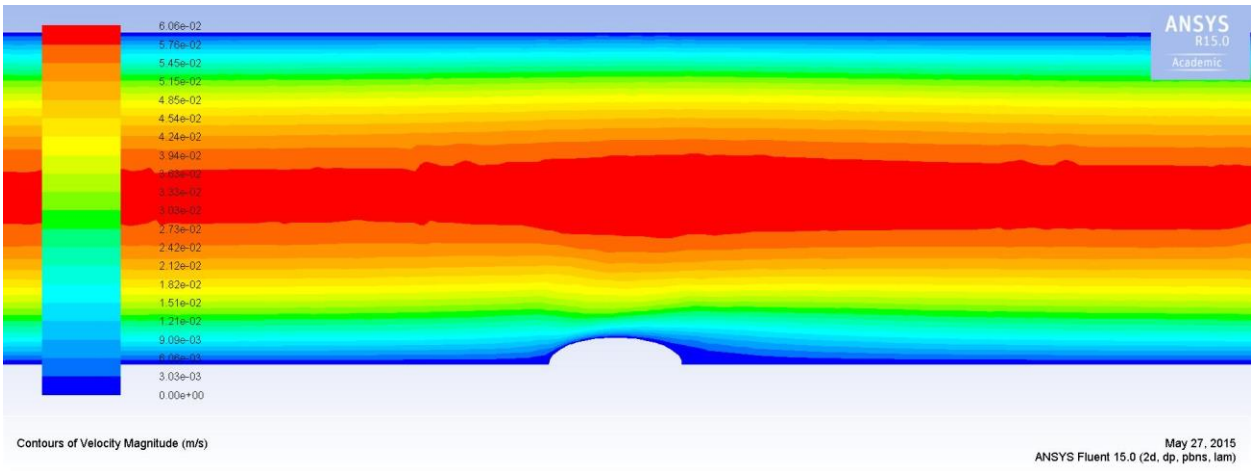

FIG 15 – Velocity contours for case 4 i.e. ‘a’ = 0.4mm & ‘b’ = 1mm.

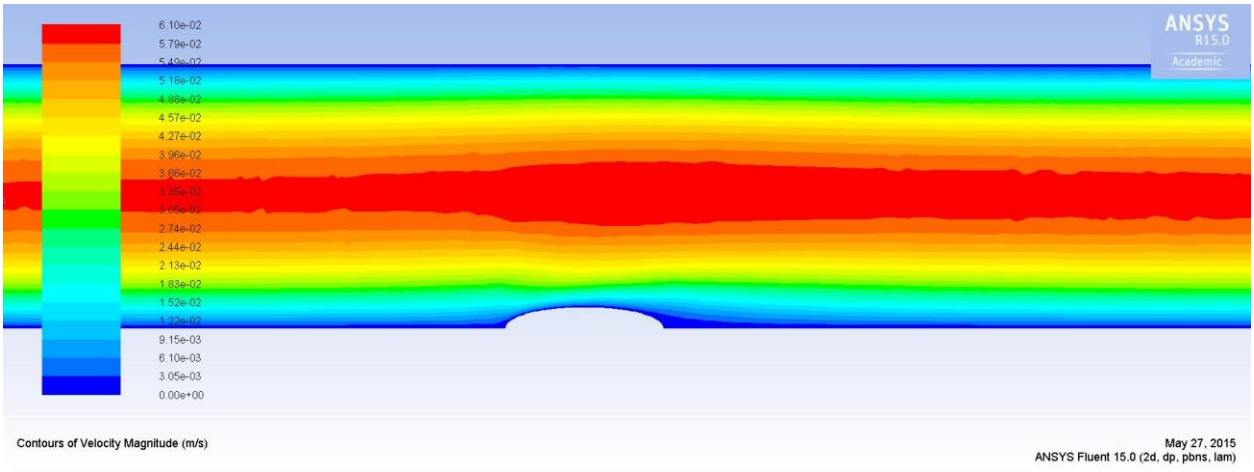

FIG 16 – Velocity contours for case 5 i.e. ‘a’ = 0.4mm & ‘b’ = 1.5mm.

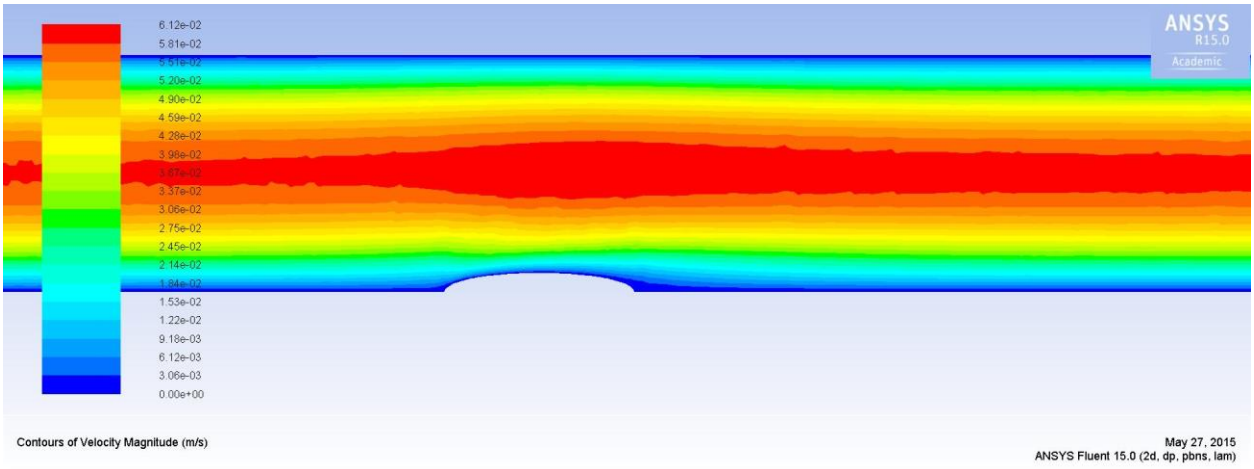

FIG 17 – Velocity contours for case 6 i.e. ‘a’ = 0.4mm & ‘b’ = 2mm.

FIG 15, 16, 17 represent the cases 4, 5, 6 when longitudinal height is 0.4mm and lateral length is 1 mm, 1.5mm, 2mm respectively. In these cases we notice some significant changes velocity profile than compared to cases 1, 2, 3. We see that the high velocity region suddenly increases in size as it reaches the obstacle. We observe that before that high velocity region is quite thin but after the obstacle it has become little thicker. We also observe that as the length is increased the velocity profile tries to regain the pattern of flat channel.

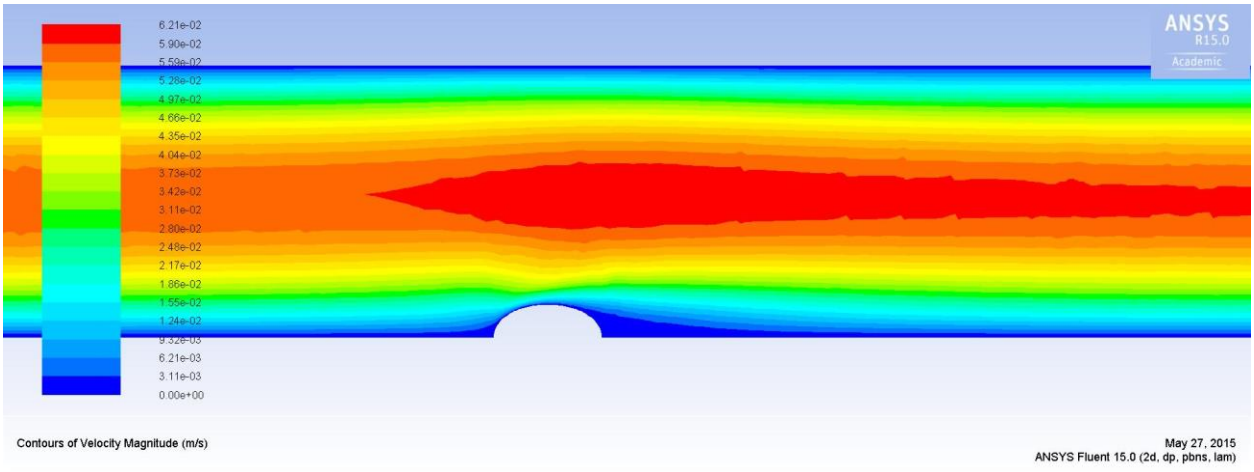

FIG 18 – Velocity contours for case 7 i.e. ‘a’ = 0.6mm & ‘b’ = 1mm.

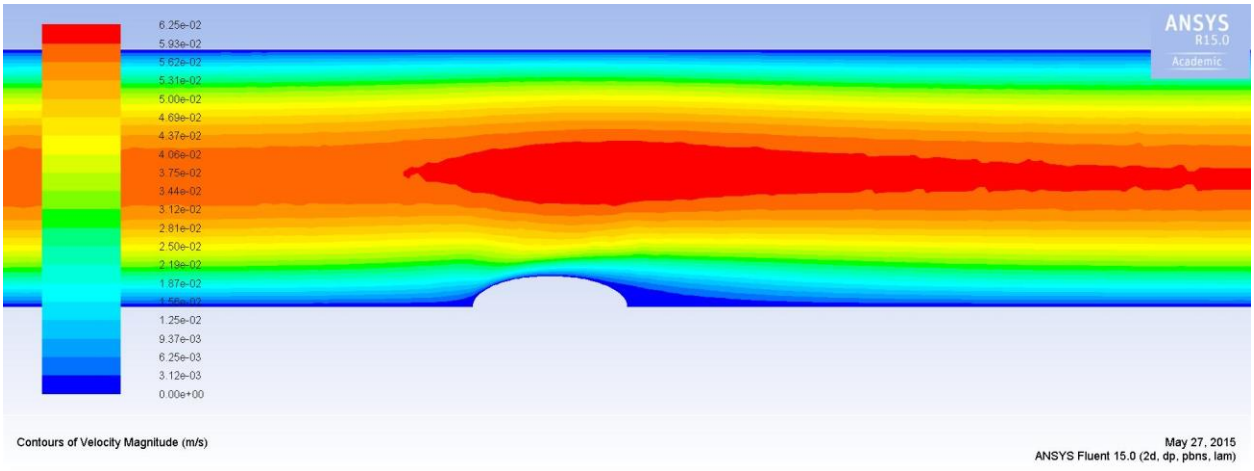

FIG 19 – Velocity contours for case 8 i.e. ‘a’ = 0.6mm & ‘b’ = 1.5mm.

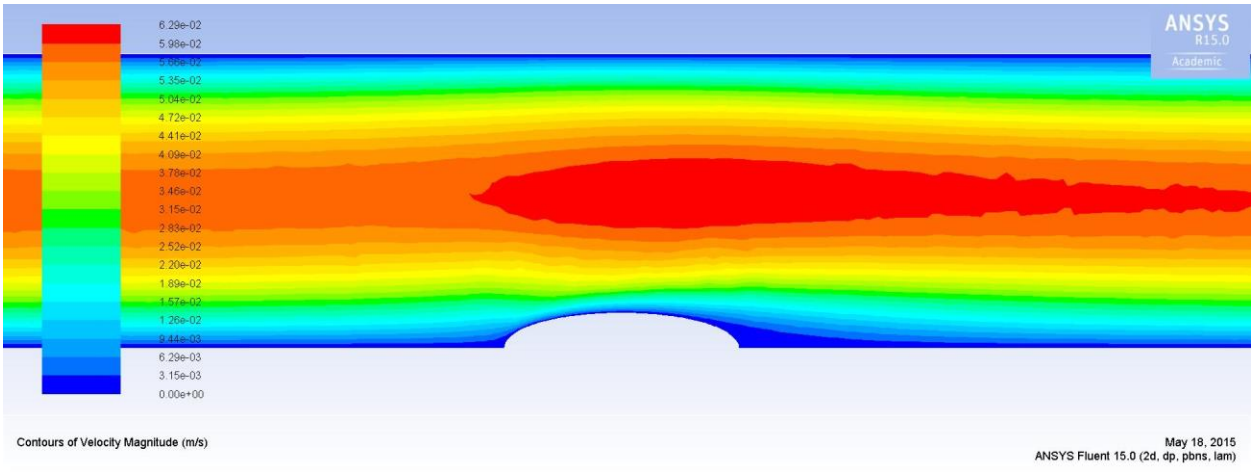

FIG 20 – Velocity contours for case 9 i.e. ‘a’ = 0.6mm & ‘b’ = 2mm.

FIG 18, 19, 20 show the velocity profile for the cases 7, 8, 9 when ‘a’ = 0.6 mm and b increases from 1 mm, 1.5mm, 2mm respectively. An important point to notice is that the high velocity region that existed before the obstacle in previous cases has disappeared. And that thickness of high velocity right above the obstacle has increased from the previous cases. Also a small low velocity region located right after the tail end of the obstacle has come in picture.

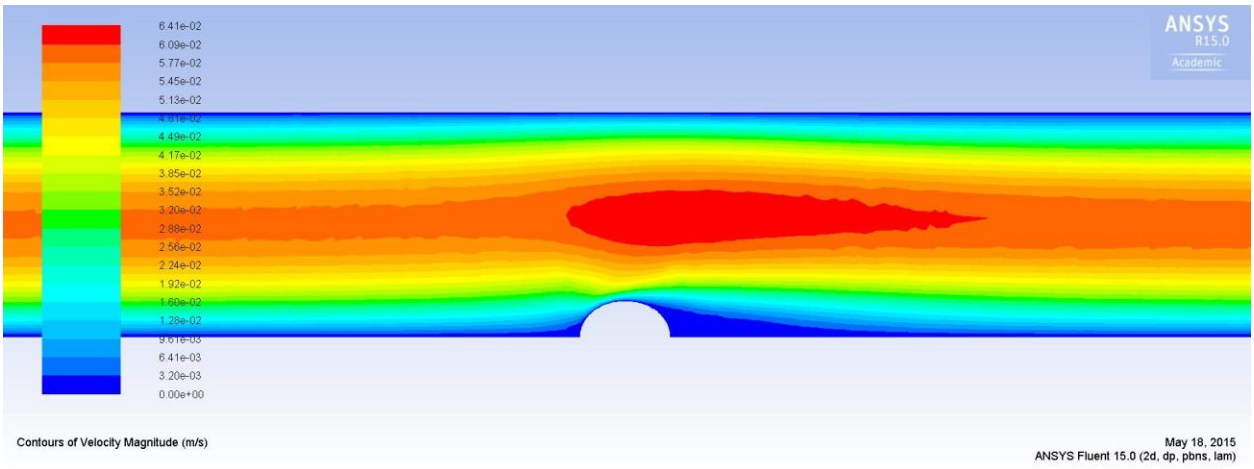

FIG 21 – Velocity contours for case 10 i.e. ‘a’ = 0.8mm & ‘b’ = 1mm.

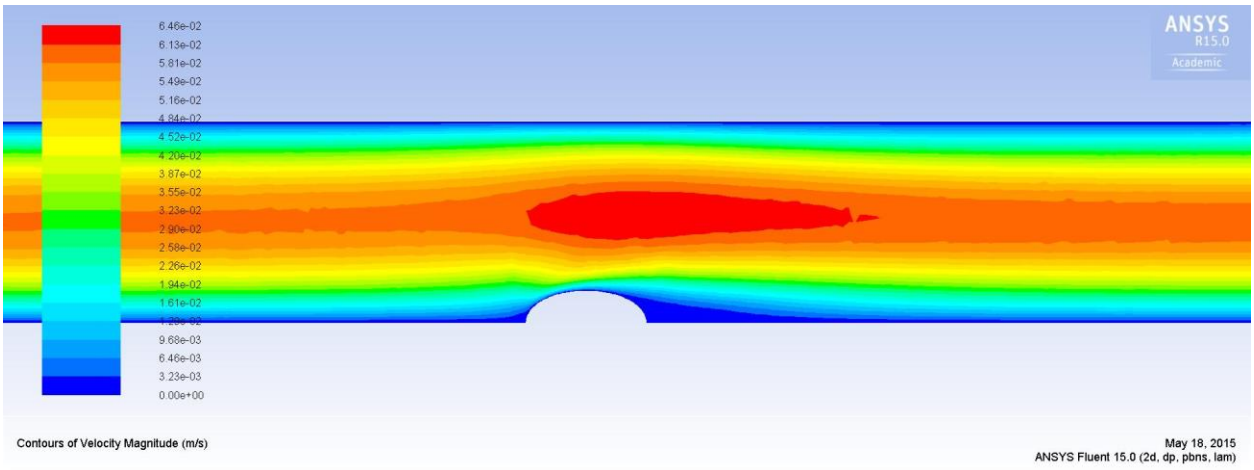

FIG 22 – Velocity contours for case 11 i.e. ‘a’ = 0.8mm & ‘b’ = 1.5mm.

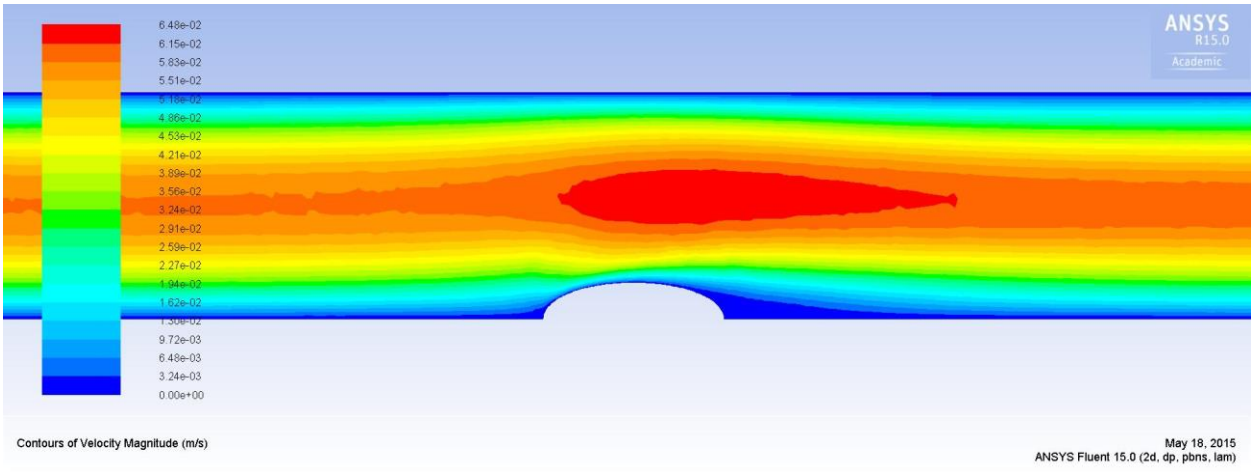

FIG 23 – Velocity contours for case 12 i.e. ‘a’ = 0.8mm & ‘b’ = 2mm.

FIG 21, 22, 23 show the velocity contour diagram for the cases 10, 11, 12 when ‘a’ = 0.8 mm and ‘b’ = 1mm, 1.5mm, 2mm respectively. The important thing to notice in these contours is that the tailing portion of the high velocity region which was extended to a longer length in previous cases has become very short. From till the outlet existence it has shrank to a few millimeters after the obstacle. Also the very low velocity region has become more significant.

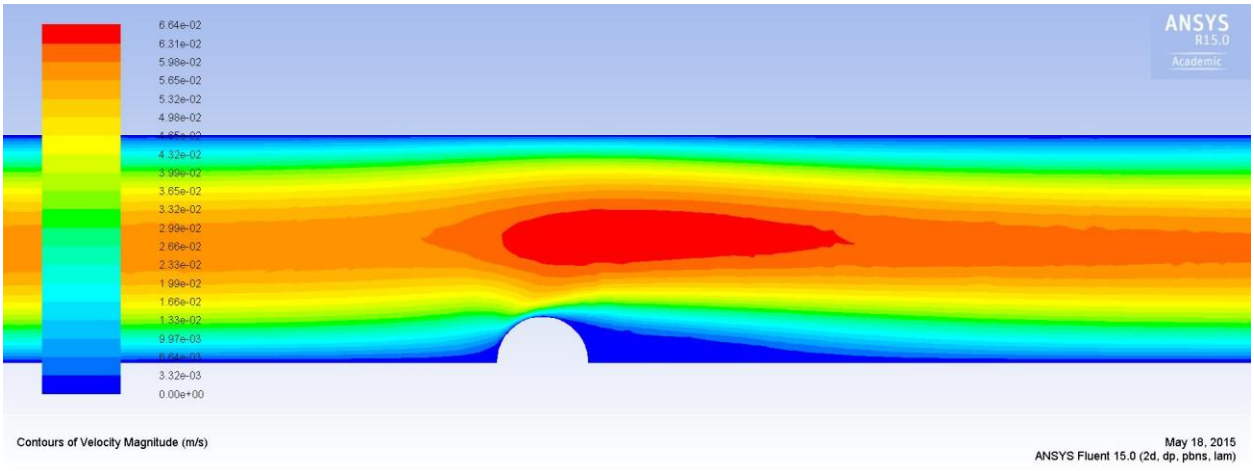

FIG 24 – Velocity contours for case 13 i.e. ‘a’ = 1mm & ‘b’ = 1mm.

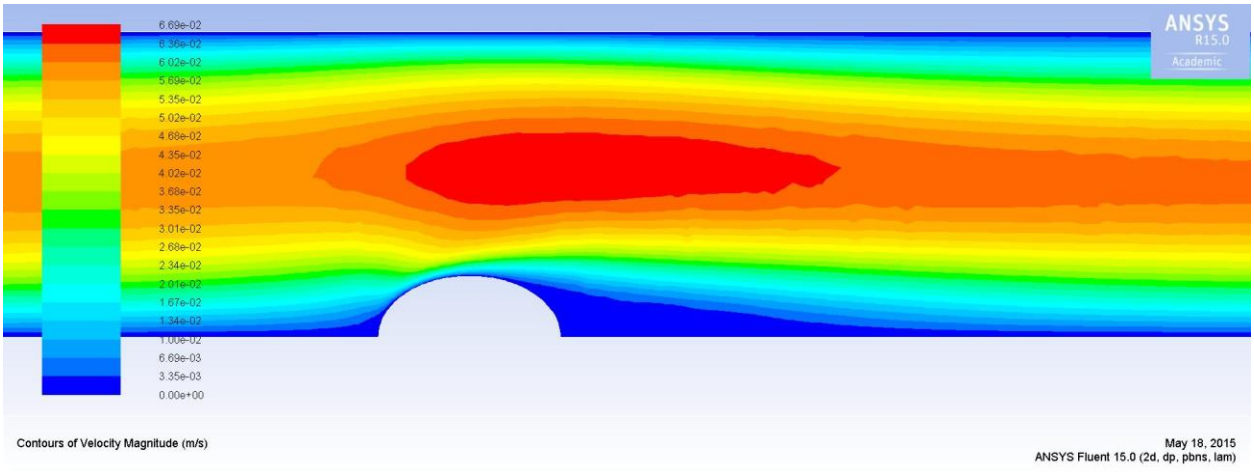

FIG 25 – Velocity contours for case 14 i.e. 'a' = 1mm & 'b' = 1.5mm.

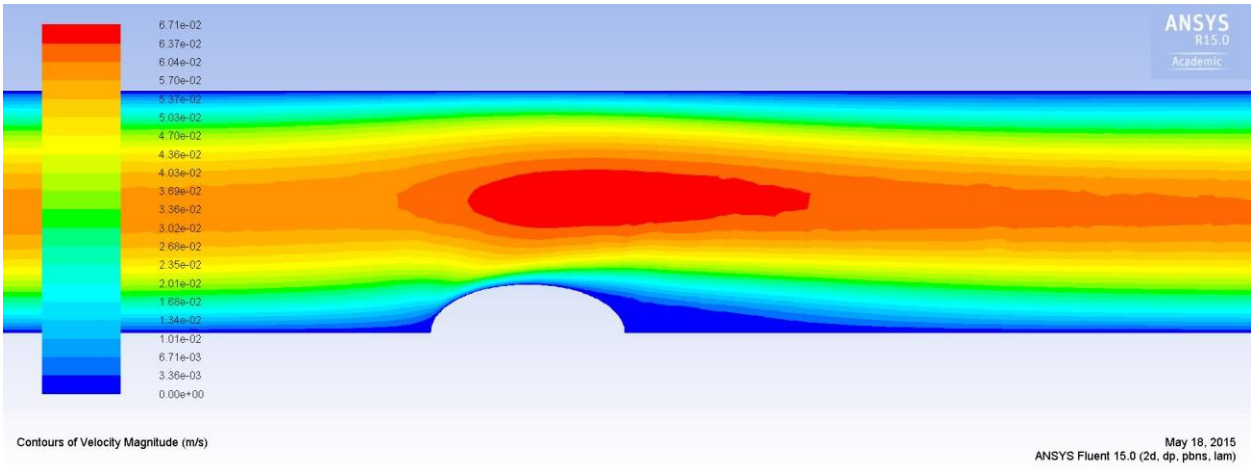

FIG 26 – Velocity contours for case 15 i.e. 'a' = 1mm & 'b' = 2mm.

FIG 24, 25, 26 show the velocity contour diagram for the cases 13, 14, 15 when 'a' = 1 mm and 'b' = 1mm, 1.5mm, 2mm respectively. The noticeable thing in these velocity contours is the high velocity region which earlier was quite large has now become a very small zone. And also the very low velocity region which was not so prominent is earlier cases has taken a significant size.

From these velocity contours for different cases we observe that the high velocity region which was formed in the flat channel was negligibly affected when the longitudinal height of obstacle was small and lateral length was large. As we can see for the case 3 with 'a' = 0.2 mm and 'b' = 2mm, the velocity contour is very similar to that of flat channel. But as the height of obstacle increases that zone of high velocity gets affected drastically.

We can easily notice that with increasing height of obstacle that high velocity zone goes on decreasing. The smallest region appearing in case 13 when 'a' = 1mm and 'b' = 1mm, in this case that zone is smallest in size whose size increases slightly when 'b' values increase in case 14 & 15.

We also observe a zone of very low velocity just after the obstacle, the region where the tail point of the obstacle meets with the channel surface. Again this zone is largest in size in case when 'a' = 1mm and 'b' = 1mm i.e. case 13. And this zone is smallest, negligible in fact, when 'a' = 0.2mm and 'b' = 2mm.

One more thing to observe is that the point from where that high velocity region starts is a little earlier than the middle point of the obstacle surface.

3.2.2 Variation of wall shear –

The wall shear values are obtained directly from the FLUENT. When these wall shear values are plotted against the point on which they are calculated we get some good significant results.

The following figures show the variation of shear stress for different geometries of obstacle with taking one dimension constant and varying the other one.

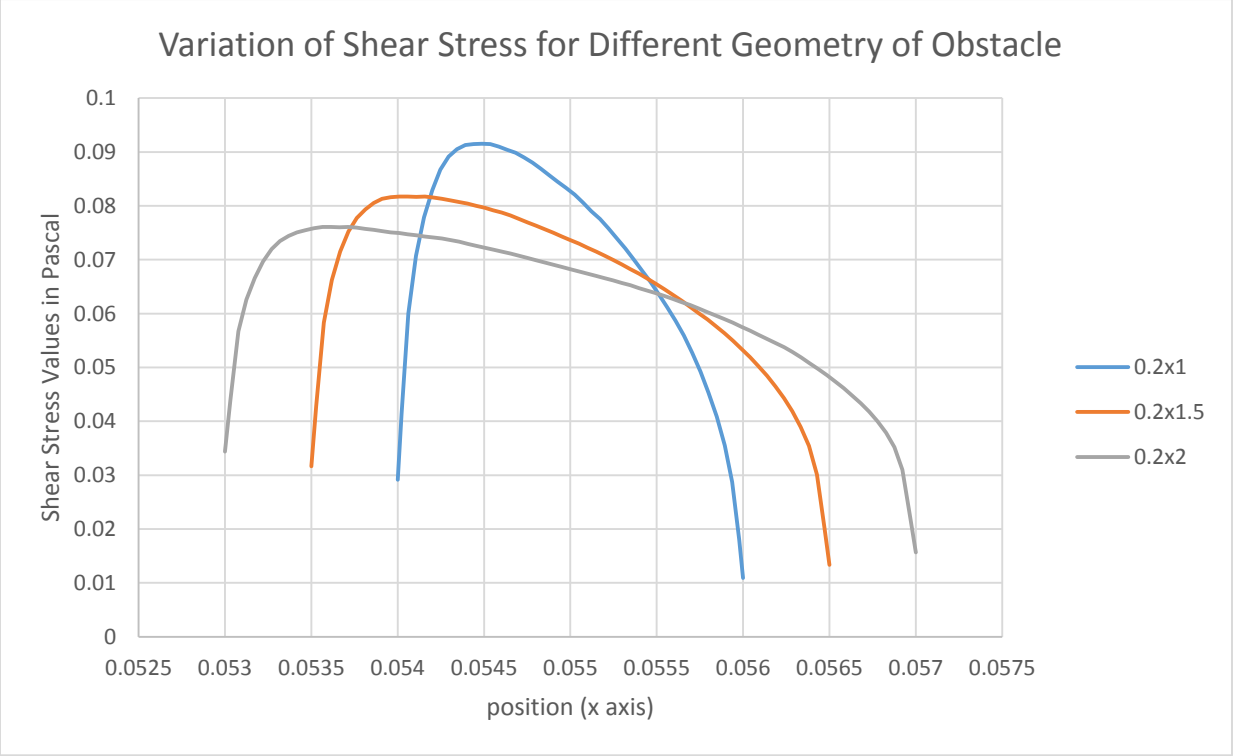

FIG 27 – Variation of shear stress with constant 'a' = 0.2mm and varying 'b'

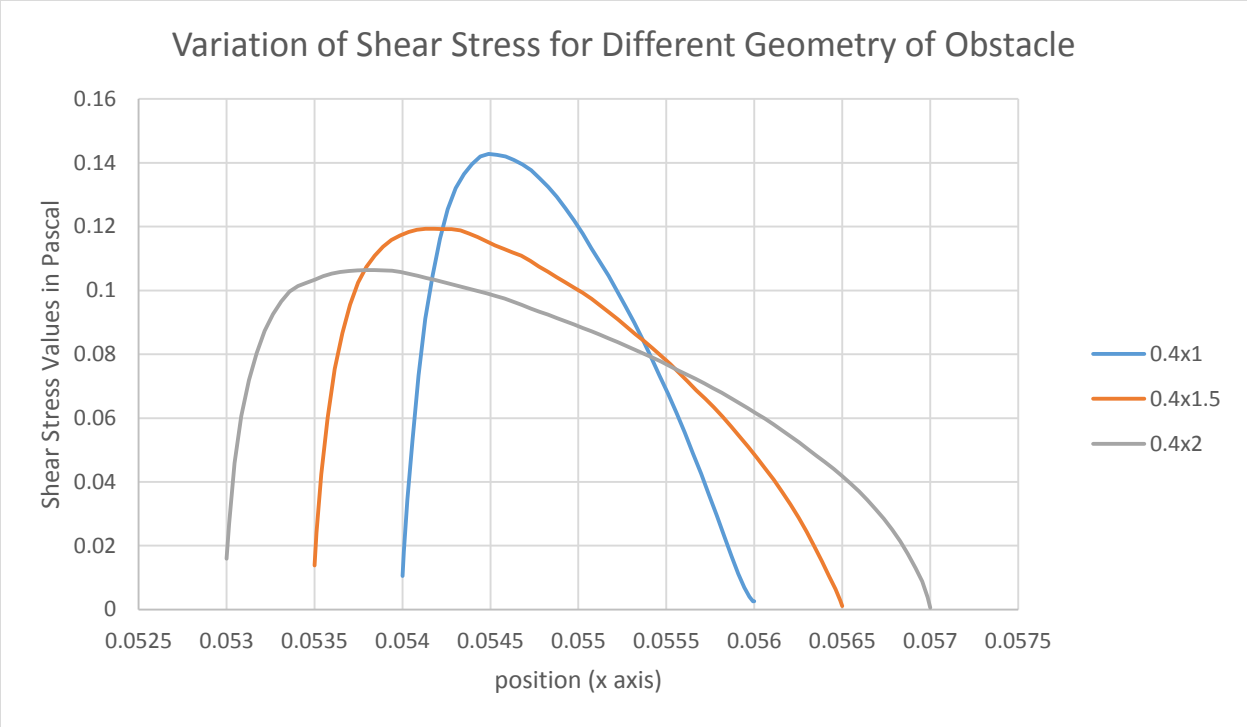

FIG 28 – Variation of shear stress with constant ‘a’ = 0.4mm and varying ‘b’

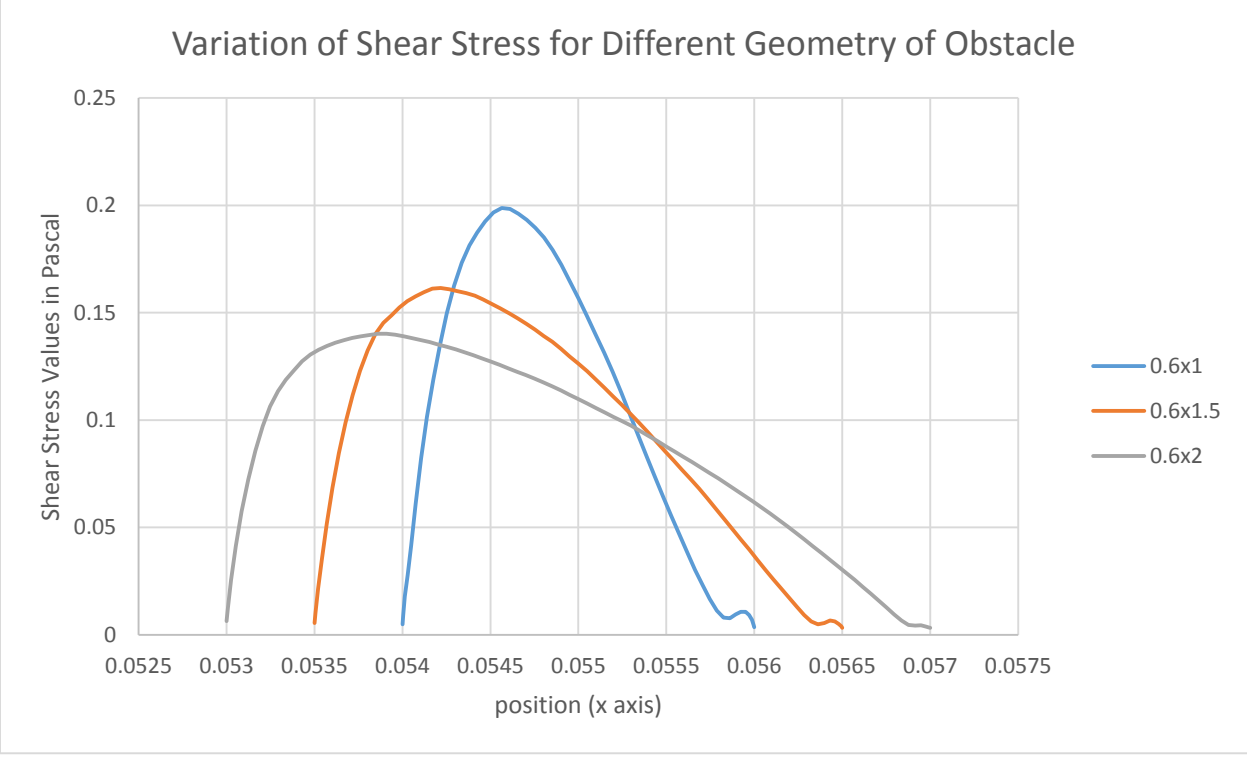

FIG 29 – Variation of shear stress with constant ‘a’ = 0.6mm and varying ‘b’

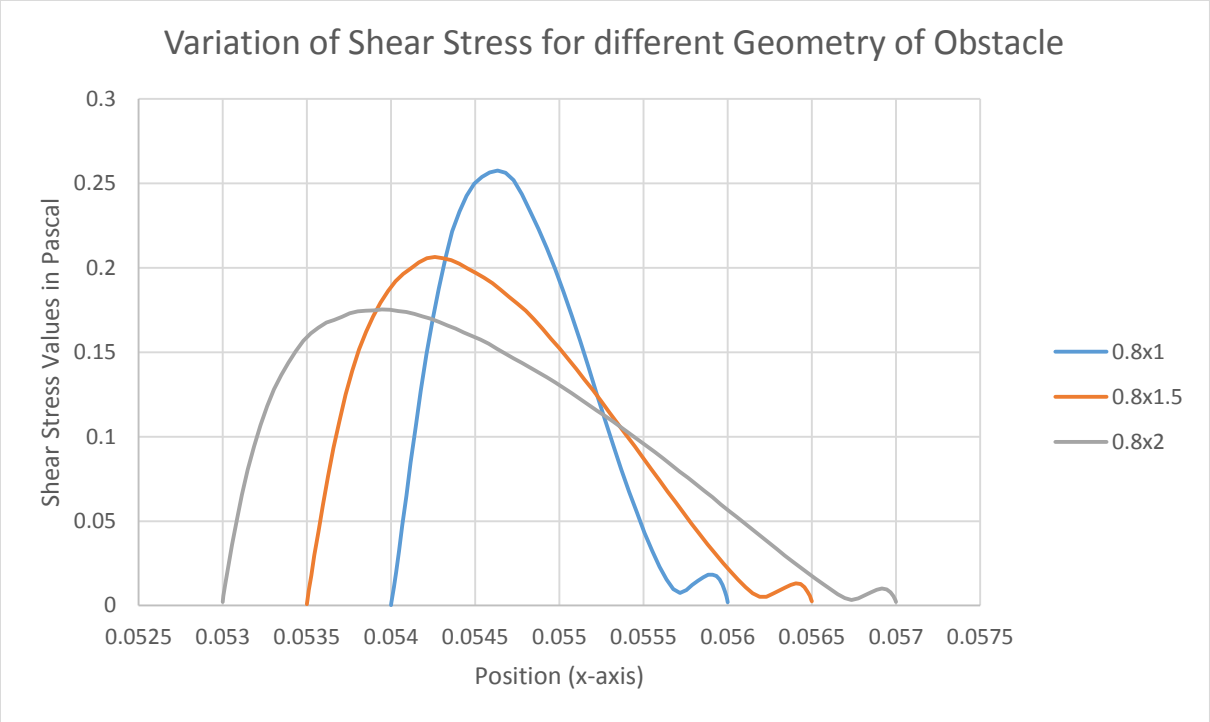

FIG 30 – Variation of shear stress with constant ‘a’ = 0.8mm and varying ‘b’

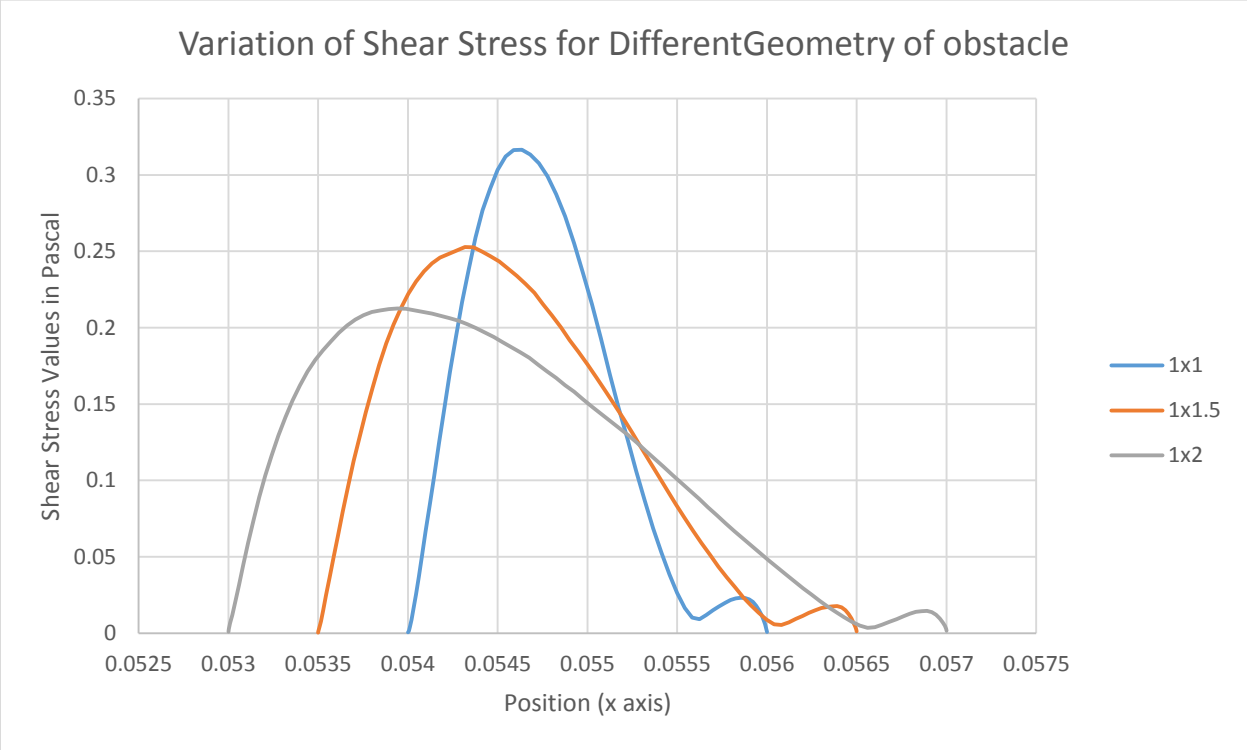

FIG 31 – Variation of shear stress with constant ‘a’ = 1mm and varying ‘b’

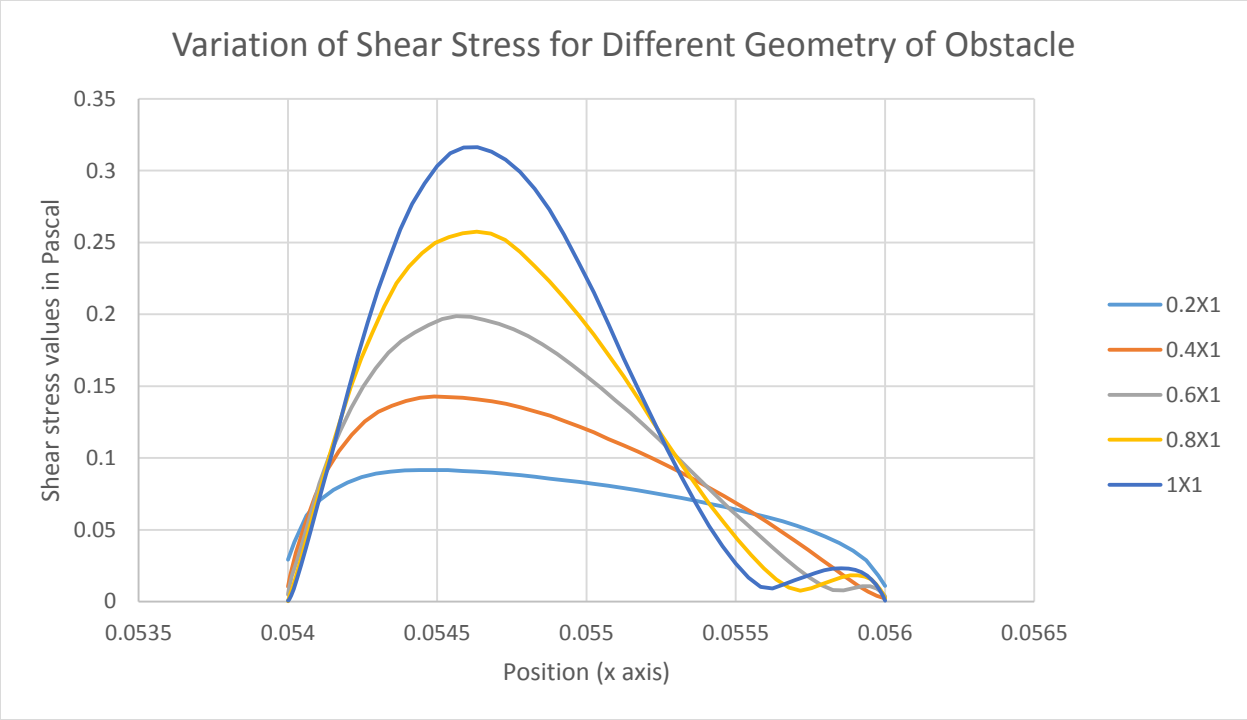

FIG 32 – Variation of shear stress with constant 'b' = 1mm and varying 'a'

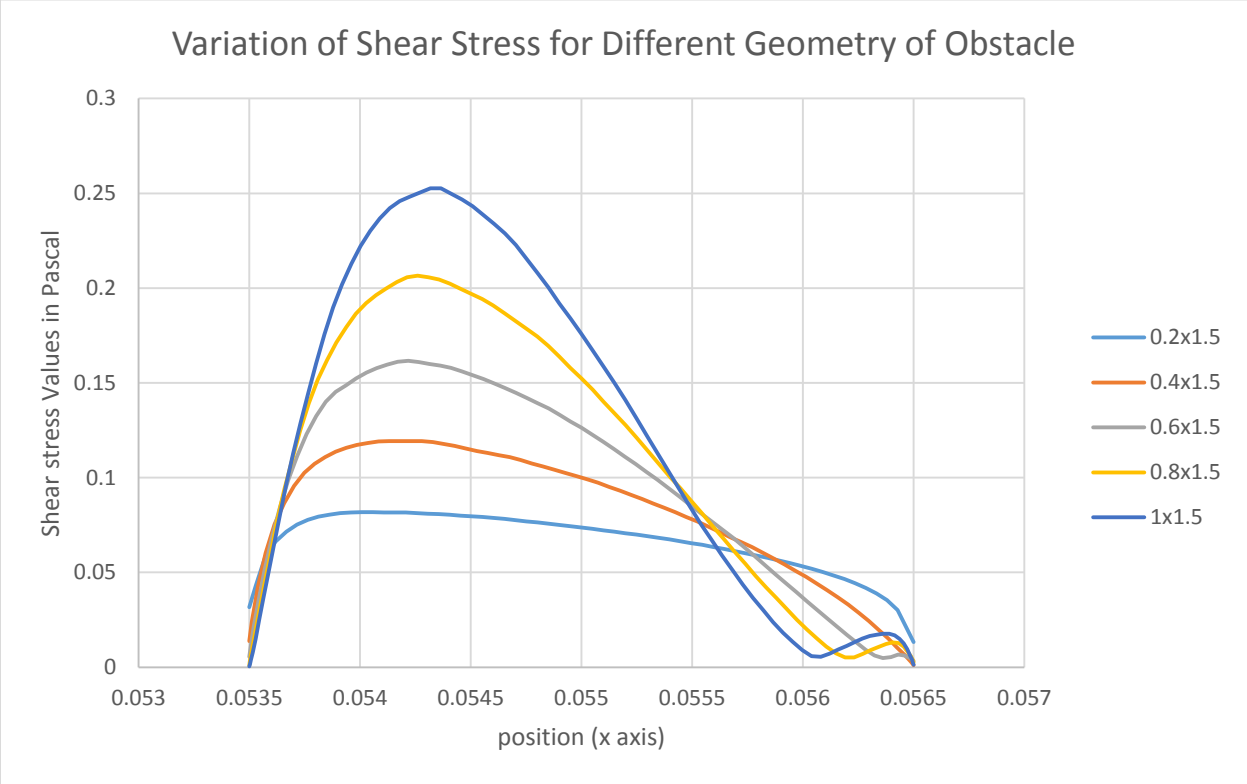

FIG 33 – Variation of shear stress with constant 'b' = 1.5mm and varying 'a'

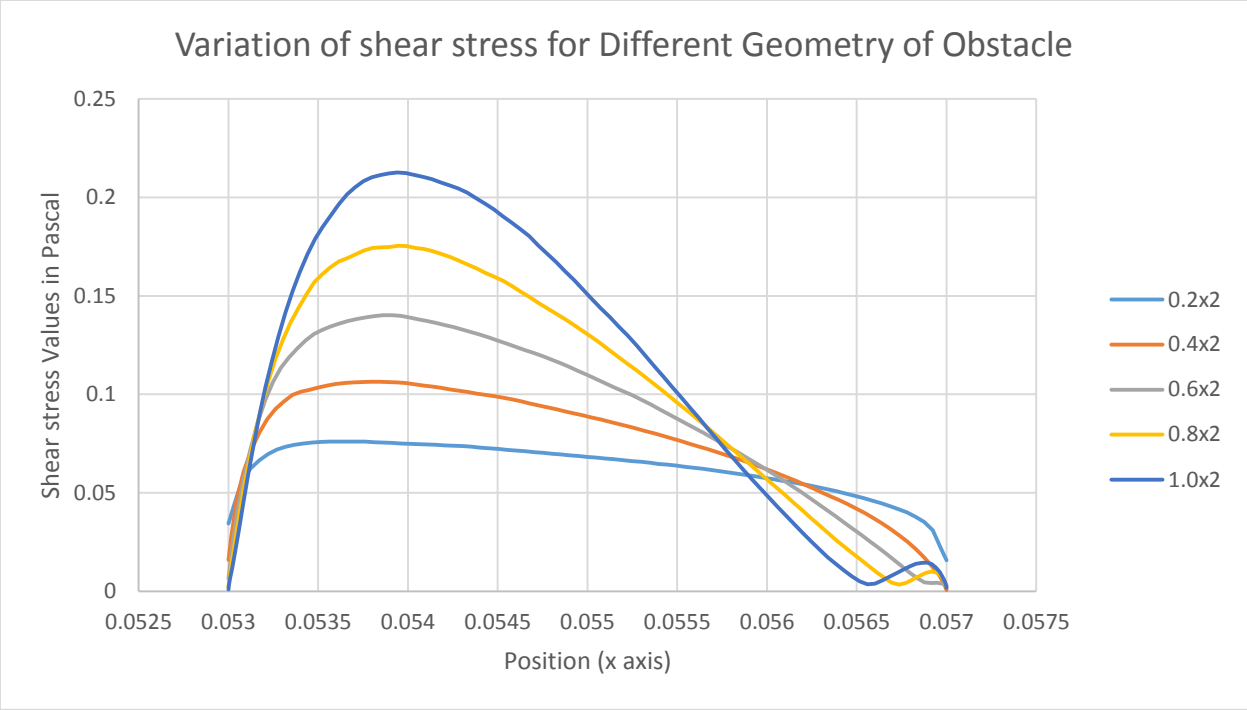

FIG 34 – Variation of shear stress with constant 'b' = 2mm and varying 'a'

When we study the variation of wall shear with changing lateral length at constant longitudinal height as shown in FIG 27 (for cases 1, 2, 3), 28(for cases 4, 5, 6), 29(for cases 7, 8, 9), 30(for cases 10, 11, 12), 31(for cases 13, 14, 15) and the variation of wall shear with changing longitudinal height at constant lateral length as shown in FIG 32 (for cases 1, 4, 7, 10,13), 33(for cases 2, 5, 8, 11, 14), 34(for cases 3, 6, 9, 12, 15) we observe –

1. The value of shear stress is less than the value of shear stress for flat plate (FIG 27-34 & 9)

2. The shear stress values decreases as the flatness of the obstacle geometry increases (FIG 27-31) (while increasing lateral length at constant longitudinal height).

3. The shear stress values increases as the height of the obstacle increases (FIG 27-31) (while increasing longitudinal height at constant lateral length).

4. The maxima of the shear stress value is a little on the left from the mid-point of obstacle surface (FIG 27-34).

5. A new secondary maxima appears (FIG 29-34).

6. The size of secondary maxima decreases as the flatness of the obstacle surface increases (FIG 29-31).

7. The graph is steeper on the leading edge side than the tailing side. (FIG 27-31).

These observations are explained as follows –

1. Since the expression for shear stress on flat plate of two parallel flat plates clearly shows the shear stress is directly proportional to the distance between the two plates. If for the most flat surface of obstacle we assume it to be perfectly flat the reduced distance between them will lead to lesser value of shear stress.

2. As we know that fluid shear stress owes its existence to viscosity which itself is the result of velocity gradient. So as the flatness of the obstacle geometry increases while its height still being constant, it approaches to the flat channel condition thus change in velocity becomes less and less which can easily be noticed from the velocity contour diagrams (FIG 12- 26) thus the shear stress value also decreases.

3. As explained in the previous case, shear stress value depends on the velocity gradient. When the height of obstacle increases at constant lateral length the velocity gradient increases rapidly which can noticed without any difficulty from the velocity contour diagrams (FIG 12-26) and also from theory we know that when an incompressible fluid flows through a region of varying cross-section the velocity is higher in the region of low cross-section. Thus the velocity gradient would be higher in case of obstacle with greater height thus it will have higher shear stress.

4. The maxima of shear stress is shifted a little towards left side because the zone of maximum velocity occurs before the maxima of obstacle.

5. The appearance of this new secondary maxima can only indicate one thing that is the wake formation. However since the size of secondary maxima not big enough the eddy formation is not observed.

6. When the obstacle becomes more and more flat then chances of eddy formation is reduced which is indicated by the gradual reduction in height of secondary maxima.

7. On the leading edge side as the flow collides with the obstacle the velocity undergoes comparatively more amount of changes than the flow when it moves past the obstacle in a zone of higher cross-sectional area.

3.3 INFERENCE –

From this study we infer one of the most prevalent rule of the nature that all objects try to achieve a stable state i.e. a state where its energy is lesser or forces on it are lesser or it is at lower potential.

We see that the wall shear is minimum in case 1 when 'a' = 0.2mm and 'b' = 2mm and the wall shear is maximum in case 13 when 'a' = 1mm and 'b' = 1mm showing that increasing flatness of an obstacle will lead to a reduction of forces acting on it.

Though it is a model where the obstacle is solid i.e. not allowed to change its shape, but it points in the direction that if it was allowed to do so it will try to achieve a position in which shear on its surface is least.

Though this model does not represent any significant phenomenon; but this study being inspired from the human endothelial cells and other such cells which are every now and then exposed to such fluid stress; shows that if a cell can achieve the shape with less longitudinal height exposed to fluid flow it can survive that fluid stresses easily.

As we noticed that shear stress values in flat channel is greater than the shear stress value in the same channel when an obstacle is there. This property can be can be used for creating special tubes from smart materials in future which can change their shape so as to minimize the shear stress thus reducing the energy lost to overcome that shear stress.

REFERENCES

1. K. Supradeepan and Roy Arnab, - Characterisation and analysis of flow over two side by side cylinders for different gaps at low Reynolds number: A numerical approach, Physics of Fluids 26, 063602 (2014); doi: 10.1063/1.4883484

2. JIANG Ren-jie. LIN Jian-zhong – Wall effects on flows past two tacndem cylinders of different diameters; Journal of Hydrodynamics, Ser. B - doi:10.1016/S1001-6058(11)60212-6

3. X.K. Wang, K. Gong, H. Liu, J.-X. Zhang, S.K. Tan; Flow around four cylinders arranged in a square configuration; Journal of Fluids and Structures 43 (2013) 179–199

4. Kyongjun Lee, Kyung-Soo Yang; Flow patterns past two circular cylinders in proximity; Computers & Fluids 38 (2009) 778–788

5. Seok-Hyun Yoon, Jae-Tack Jeong; Stokes flow through a microchannel obstructed by a vertical plate; European Journal of Mechanics B/Fluids 34 (2012) 64–69

6. Hyeon-Seok Seo, Youn-Jea Kim; A study on the mixing characteristics in a hybrid type microchannel with various obstacle configurations; Materials Research Bulletin 47 (2012) 2948–2951

7 Muammer Ozgoren , Abdulkerim Okbaz, Sercan Dogan, Besir Sahin, Huseyin Akilli; Investigation of flow characteristics around a sphere placed in a boundary layer over a flat plate; Experimental Thermal and Fluid Science 44 (2013) 62–74

8 Min-Hsing Chang, Falin Chen, Nai-Siang Fang; Analysis of membraneless fuel cell using laminar flow in a Y-shaped microchannel; Journal of Power Sources 159 (2006) 810–816

9 Malboubi, M., Jayo, A., Parsons, M., Charras, G. ; An open access microfluidic device for the study of the physical limits of cancer cell deformation during migration in confined environments (Article) ; Microelectronic Engineering ; Volume 144, 16 August 2015, Pages 42-45

10 Daniel A. Hammer and Sachin M. Apte ; Simulation of cell rolling and adhesion on surfaces in shear flow : general results and analysis of selectin-mediated neutrophil adhesion ; Biophys. J. Biophysical Society; Volume 63 July 1992 35-57

11 Olivier Tissot, Anne Pierres, Colette Foa, Michel Delaage, and Pierre Bongrand ; Motion of cells sedimenting on a solid surface in a laminar shear flow ; Biophys. J. © Biophysical Society Volume 61 January 1992 204-215

12 Yiannis S. Chatzizisis, Ahmet Umit Coskun, Michael Jonas, Elazer R. Edelman, Charles L. Feldman, Peter H. Stone ; Role of Endothelial Shear Stress in the Natural History of Coronary Atherosclerosis and Vascular Remodeling ; Journal of the American College of Cardiology ; Vol. 49, No. 25, 2007

13 E. GAVZE and M. SHAPIRO PARTICLES IN A SHEAR FLOW NEAR A SOLID WALL: EFFECT OF NONSPHERICITY ON FORCES AND VELOCITIES ; *Int. J. Multiphase Flow* Vol. 23, No. 1, pp. 155 182, 1997

14 N.-E. Sabiri, R.P. Chhabra , J. Comiti , A. Montillet ; Measurement of shear rate on the surface of a cylinder submerged in laminar flow of power-law fluids ; Experimental Thermal and Fluid Science 39 (2012) 167–175

15 Katsuko Sakai Furukawa, Takashi Ushida, Takayuki Nagase, Hideki Nakamigawa, Takuya Noguchi, Tamotsu Tamaki, Junzo Tanaka, Tetsuya Tateishi ; Quantitative analysis of cell detachment by shear stress ; Materials Science and Engineering C 17 Ž2001. 55–58

16 Donald P. Gaver, III, and Stephanie M. Kute ; A Theoretical Model Study of the Influence of Fluid Stresses on a Cell Adhering to a Microchannel Wall ; Biophysical Journal Volume 75 August 1998 721–733

17 Harvey A. R. Williams, Lisa J. Fauci, Donald P. Gaver III ; EVALUATION OF INTERFACIAL FLUID DYNAMICAL STRESSES USING THE IMMERSED BOUNDARY METHOD ; Discrete Continuous Dyn Syst Ser B. 2009 March 1; 11(2): 519–540.

18 A. L. Hazel and T. J. Pedley ; Vascular Endothelial Cells Minimize the Total Force on Their Nuclei ; Biophysical Journal Volume 78 January 2000 47–54